

STRENGTH OF THIN WALLED CYLINDERS SUBJECTED TO
COMBINED COMPRESSION AND TORSION

Thesis by
James E. Lipp

In Partial Fulfillment of the Requirements for the Degree of
Doctor of Philosophy

California Institute of Technology
Pasadena, California

1935

TABLE OF CONTENTS

| | <u>Page</u> |
|---|-------------|
| Summary | 1 |
| Results and Conclusions | 2 |
| Introduction | 3 |
| Empirical $K\phi$ Curves | 5 |
| Theoretical $K\phi$ Curve | 14 |
| Experimental Results | 24 |
| Coordination of Theory with Experiment | 28 |
| Acknowledgment | 30 |
| References | 31 |
| Notation | 32 |
| Experimental Data | 34 |
| Illustrations | |
| 1. Bridget's Curve | 4 |
| 2. Combined Stresses | 6 |
| 3. Failure of Cylinder | 7 |
| 4. Effective Radius | 8 |
| 5. σ , vs. τ , | 13a |
| 6. $K\phi$ vs. ϕ Empirical | 13b |
| 7. Sheet Element | 15 |
| 8. Effect of Compression | 16 |
| 9. Relation of ϵ_c to λ and R' | 17 |

TABLE OF CONTENTS (cont'd)

| | <u>Page</u> |
|---------------------------------------|-------------|
| 10. Effect of Tension | 17 |
| 11. $K\phi$ vs. ϕ Theoretical | 23a |
| 12. N vs. $\frac{Y_r}{E_t}$ Empirical | 29a |
| Experimental Curves | 38a |

I. SUMMARY:

This thesis is an extension of the work which was started by Dr. Donnell and Lieutenant Bridget on the problem of thin metal cylinders under combined torsion and direct stress. An explanation of the shape of the compression vs. torsion curve is found by calculating the yield failure of an element of sheet considered as a column with both transverse and end loads. Several causes of variation in that curve shape have been brought to light, but must wait for very complete and accurate experiments or a complete theoretical treatment for verification.

Experiments have been extended to several new materials, and have given results which parallel the previous work on steel. In order to cover as wide a range of cylinders as possible, the data of reference no. 1 have been included with the present series of tests.

II. RESULTS AND CONCLUSIONS:

(1) Theory and experiment both confirm the form of the curve:

$$1 - \frac{\sigma}{\sigma_0} = \left(\frac{\tau}{\tau_0} \right)^n$$

where σ_0 = failure stress, pure compression

τ_0 = " " , " torsion

for cylinders of all thicknesses and materials.

(2) The value of the exponent n is shown to depend largely upon the value of the parameter $\frac{Y}{E} \frac{r}{t}$

where Y = yield stress of the material

E = Young's Modulus

r = radius

t = thickness

(3) A mean curve of n vs. $\frac{Y}{E} \frac{r}{t}$ (empirical) is recommended for design.

(4) The equations developed in this paper indicate that there is probably no scale effect in the value of n. Results of these small scale experiments can, therefore, be applied directly to full scale work.

III. INTRODUCTION:

Several years ago, Dr. L. H. Donnell, then at the Institute, started the investigation of thin walled cylinders of various types of cross-section shape and reinforcement under combinations of compression, torsion and bending. Work is still in the first and simplest stages. Unreinforced circular cylinders have been considered in pure torsion, pure compression and pure bending by Donnell himself (ref. 2,3). Lieutenant Bridget's paper (ref. 1) and the present thesis give the case of a combination of compression and torsion.

Bridget's work was the starting point of this particular discussion and will, therefore, be summarized very briefly.

Six series of tests on steel cylinders (and one series of brass) of various sizes showed that a plot of compression vs. torsion at failure gives a curve of the form (fig. 1a)

$$1 - \sigma = \tau^n$$

If σ_0 = compression stress for failure in pure compression, and τ_0 = torsion (shear) stress for pure torsion failure, then

$$1 - \frac{\sigma}{\sigma_0} = \left(\frac{\tau}{\tau_0} \right)^n \quad (1)$$

(Fig. 1b) gives a dimensionless form of the curve.

An "intuitive" explanation was given. The curve must be symmetrical about the compression axis and must also be continuous. Therefore the slope must be zero at $\sigma = \sigma_0$, $\tau = 0$. Tension increases the resistance of the wall to compression failure. Therefore the slope is negative at $\sigma = 0$, $\tau = \tau_0$. A smooth curve which fits both of the conditions has the shape that is given by experiment.

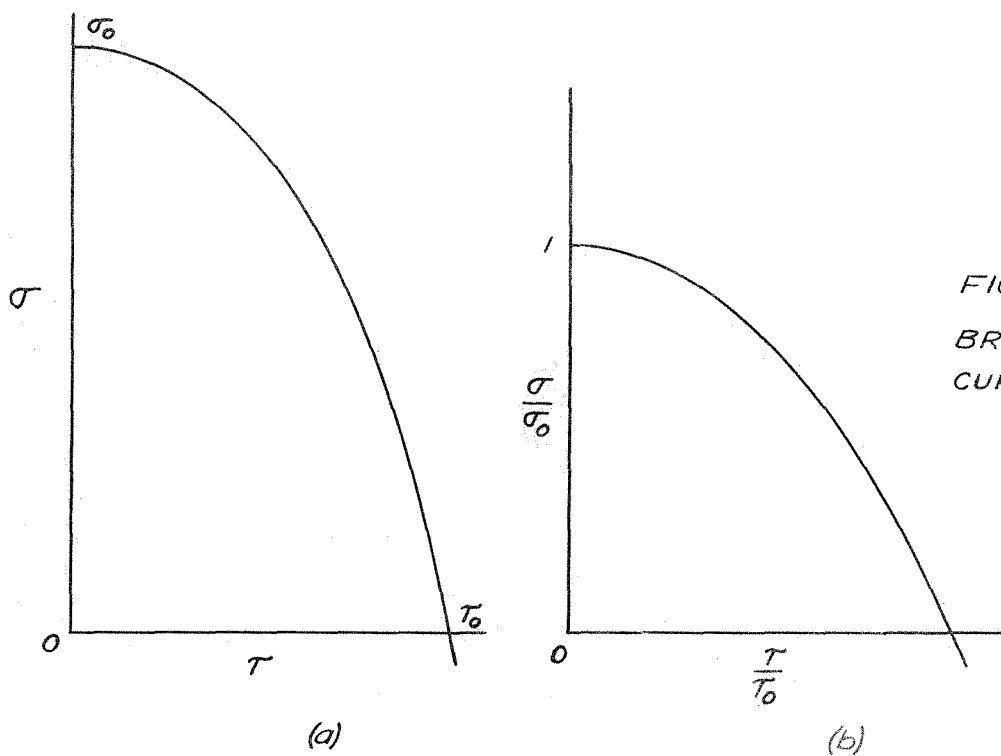


FIG. 1.
BRIDGET'S
CURVE

IV. EMPIRICAL $K\phi$ CURVES:

In order to consider the problem more in detail, it is necessary to calculate the stresses which occur within the cylinder walls. To do this, we note that failure is a wave phenomenon, i.e. the sheet fails in compression. We must, therefore, study the resistance of the wall to buckling in compression for the case in which the principal compression does not act parallel to the elements of the cylinder. Dimensionless parameters are used wherever possible in the analysis. The present section is used to develop a dimensionless curve (in an explainable form) for "resistance" vs. "angle of principal stress" from the empirical relation (1). A future section will attempt to explain the curve obtained. See page 32 for notation.

(a) Principal Compression Stress.

For an element of sheet acted upon by forces σ_u , σ_v and τ_{uv} (fig. 2), we know that the directions of principal stresses are given by:

$$\tan 2\mu = \frac{2\tau_{uv}}{\sigma_u - \sigma_v} \quad (2)$$

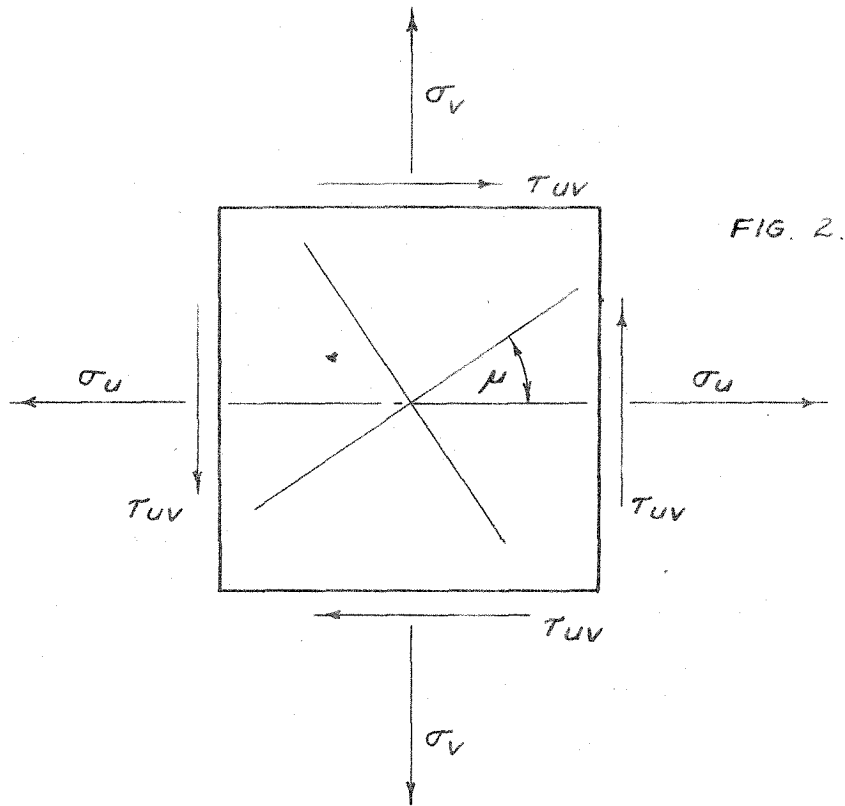


FIG. 2.

In the case of a cylinder under combined compression and torsion, the stresses above become $\sigma_u = 0$, $\sigma_v = -\sigma_y$ (compression now assumed to be positive) and $\tau_{uv} = \tau$. Only one of the two principal axes is of interest (compression). Therefore:

$$\tan 2\phi = \frac{2\tau}{\sigma_y} \quad 0 < \phi < 45^\circ \quad (3)$$

where ϕ = angle between principal compression and element of cylinder.

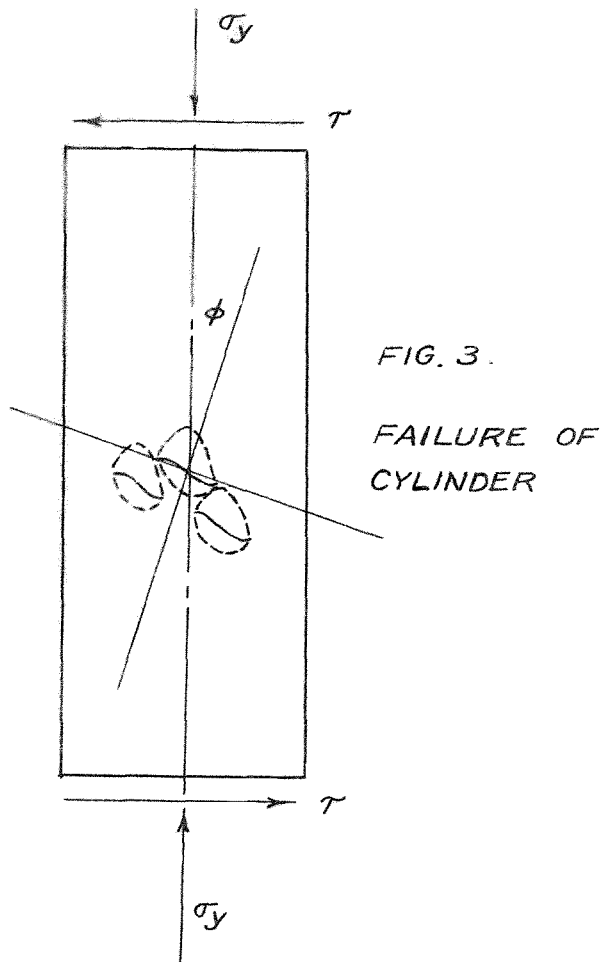


FIG. 3.
FAILURE OF
CYLINDER

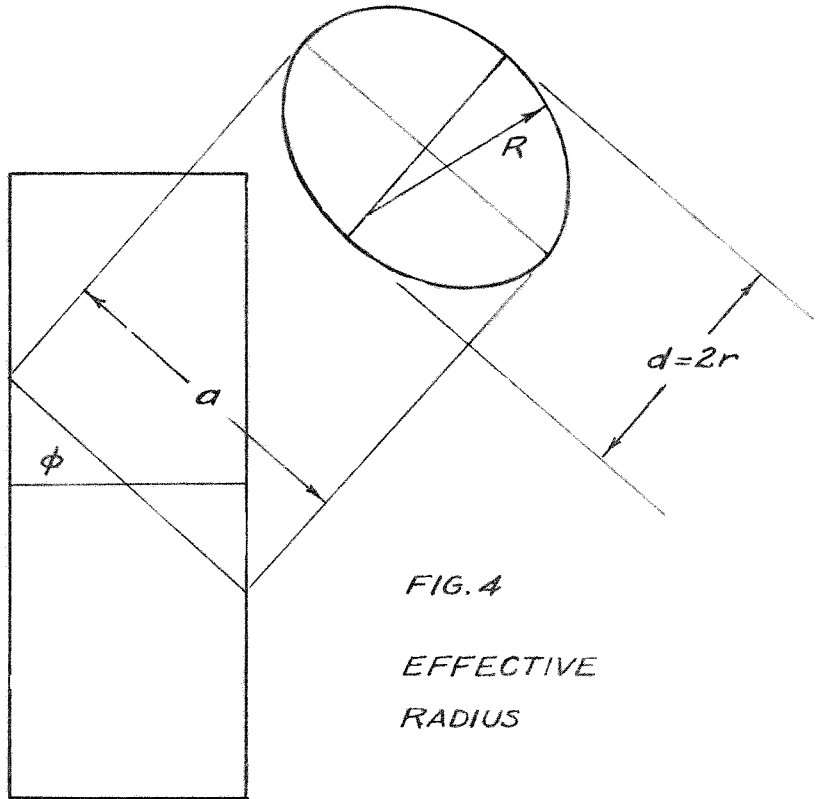
The general equation for principal stress (in the ϕ direction) reduces to:

$$\sigma_{\phi} = \sigma_y \cos^2 \phi + 2\tau \cos \phi \sin \phi$$

(b) "Effective" Radius.

It will be assumed, and experiment verifies the assumption, that for medium length cylinders buckling waves form nearly perpendicular to the direction ϕ , as shown in fig. 3. The maximum radius (i.e. the place at which buckling starts in the plane of a wave) is the maximum radius of an elliptical section taken at the angle ϕ with the base of the cylinder. Such an elliptical section is shown in fig. 4.

The minor axis will be \underline{d} , the diameter of the cylinder;
 and the major axis, \underline{a} , will be $a = \frac{d}{\cos\phi}$



From the properties of an ellipse:

$$R = \frac{a^2}{2d} = \frac{r}{\cos^2\phi} \quad (5)$$

(c) Idea of $K\phi$.

A simple compression stress acting parallel to the elements of a sheet that is singly curved to the radius R is exactly the case of a cylinder under pure compression. This suggests the method of comparing σ_ϕ in the actual cylinder with

σ_0 for a cylinder of radius R (same material).

In order to do this, write:

$$\sigma_\phi = K\phi \frac{Et}{r} \quad (6)$$

This type of expression has been found to apply to both pure compression and pure torsion to a very fair approximation. A short discussion of this point is necessary here.

For compression, the generally accepted relation is

$$\sigma_0 = .3 \frac{Et}{r} \quad \text{i.e.} \quad K\phi = .3 \quad \text{at} \quad \phi = 0 \quad (7)$$

The constant is empirical. "Classical" stability theories give $K(\phi = 0)$ as having various constant values from (.3) to (.6), (see ref. 4). Donnell's large deflection theory gives a somewhat lower value (about .2). In any event, the theories are all fairly well agreed on the form of equation 7.

In torsion we have:

$$\tau_0 = .075 \frac{Et}{r} \quad (8)$$

This is applicable only to cylinders such as are usually found in aeronautical structures. Extremely long or extremely short cylinders must be calculated by Donnell's formula (ref. 2).

Experiments both at Berkeley and here agree very well with the constant (.075).

Noting that $\phi = 45^\circ$ for pure torsion, we can calculate K_ϕ for this case.

$$\sigma_\phi = 2\tau \cos 45^\circ \sin 45^\circ = \tau$$

$$R = \frac{r}{\cos^2 45^\circ} = 2r$$

$$\therefore \sigma_\phi = K_\phi \frac{Et}{R} = K_\phi \frac{Et}{2r} = \tau = .075 \frac{Et}{r}$$

$$\therefore K_\phi = .15 \text{ for } \phi = 45^\circ$$

Since equation (6) holds for compression and torsion separately, it is assumed to be valid for combined compression and torsion.

(d) Empirical K_ϕ vs. ϕ .

The following equations have now been obtained:

$$\tan 2\phi = \frac{2\tau}{\sigma_y} \quad 0 < \phi < 45^\circ \quad (3)$$

$$\sigma_\phi = \sigma_y \cos^2 \phi + 2\tau \cos \phi \sin \phi \quad (4)$$

$$R = \frac{r}{\cos^2 \phi} \quad (5)$$

$$\sigma_\phi = K_\phi \frac{Et}{R} \quad (6)$$

For any relation $\sigma_y = f_1(\tau)$ it is, therefore, possible to find a corresponding relation $K_\phi = f_2(\phi)$. Bridget's equation:

$$1 - \frac{\sigma_y}{\sigma_0} = \left(\frac{\tau}{\tau_0}\right)^n$$

where

$$\sigma_0 = .3 \frac{Et}{r}, \quad \tau_0 = .075 \frac{Et}{r}$$

will thus lead to an empirical curve of $K\phi$ vs. ϕ for a given value of n . Two characteristic values of the exponent n will be considered: Case I, $n = 3$ (curve I, fig. 5) and Case II, $n = 2$ (curve II, fig. 5).

Case I: $n = 3$

Combine equations (4), (5) and (6):

$$\therefore K\phi \frac{Et}{r} = \sigma_y + 2\tau \tan \phi$$

Equation (3) leads to the formula:

$$\tan \phi = \frac{(4\tau^2 + \sigma_y^2)^{\frac{1}{2}} - \sigma_y}{2\tau}$$

$$\begin{aligned} \therefore K\phi \frac{Et}{r} &= \sigma_y + \frac{2\tau [(4\tau^2 + \sigma_y^2)^{\frac{1}{2}} - \sigma_y]}{2\tau} \\ &= (4\tau^2 + \sigma_y^2)^{\frac{1}{2}} \end{aligned}$$

Write:

$$\tau = \tau_0 \frac{\tau}{\tau_0} = .075 \frac{Et}{r} \tau_1$$

$$\sigma_y = \sigma_0 \frac{\sigma_y}{\sigma_0} = .3 \frac{Et}{r} \sigma_1$$

$$\therefore K\phi = .15 (\tau_1^2 + 4\sigma_1^2)^{\frac{1}{2}} \quad (9)$$

Now introduce the equation for this particular case:

$$1 - \sigma_1 = \tau_1^3 \quad (10)$$

Equations (9) and (10) give:

$$K\phi = .15 (4\tau_1^6 - 8\tau_1^3 + \tau_1^2 + 4)^{\frac{1}{2}} \quad (11)$$

Equation (3) can be written:

$$\tan 2\phi = \frac{2\tau}{\sigma_y} = \frac{\tau_1}{2\sigma_1}$$

$$\therefore \tan 2\phi = \frac{\tau_1}{2(1-\tau_1^3)} \quad (12)$$

Equations (11) and (12) are a pair of parametric equations between $K\phi$, ϕ and τ_1 . By assigning values to τ_1 between 0 and 1, the curve $K\phi$ vs. ϕ for $n = 3$ is plotted (curve I, fig. 6).

| | | | | | | | | | | | |
|------|------|------|------|------|-------|-------|-------|-------|-------|-------|-----|
| .1 | .2 | .3 | .4 | .5 | .6 | .7 | .8 | .9 | .94 | .97 | 1.0 |
| .3 | .299 | .295 | .287 | .273 | .252 | .223 | .191 | .163 | .149 | .147 | .15 |
| 1.5° | 2.8° | 4.5° | 6.0° | 8.3° | 10.5° | 14.0° | 19.6° | 29.5° | 34.9° | 39.8° | 45° |

Case II, $n = 2$

In this, just as in Case I, we get equation (9):

$$K\phi = .15 (\tau_1^2 + 4\sigma_1^2)^{\frac{1}{2}} \quad (9)$$

Instead of equation (10) use:

$$1 - \sigma_1 = \tau_1^2 \quad (13)$$

$$\therefore K\phi = .15 (4\tau_1^4 - 7\tau_1^2 + 4)^{\frac{1}{2}} \quad (14)$$

$$\tan 2\phi = \frac{\tau_1}{2(1-\tau_1^2)} \quad (15)$$

Equations (14) and (15) are handled the same as (11) and (12).

See curve II, fig. 6.

| | | | | | | | | | | | |
|------|------|------|------|------|-------|-------|------|-------|------|-------|-----|
| .1 | .2 | .3 | .4 | .5 | .6 | .7 | .8 | .9 | .94 | .97 | 1.0 |
| .297 | .289 | .277 | .259 | .237 | .212 | .186 | .162 | .147 | .145 | .146 | .15 |
| 1.5° | 3° | 4.7° | 6.7° | 9.2° | 12.5° | 17.2° | 24° | 33.6° | 38° | 41.5° | 45° |

FIG 5 σ_1 vs. T_1

CURVE I $N=3$

CURVE II $N=2$

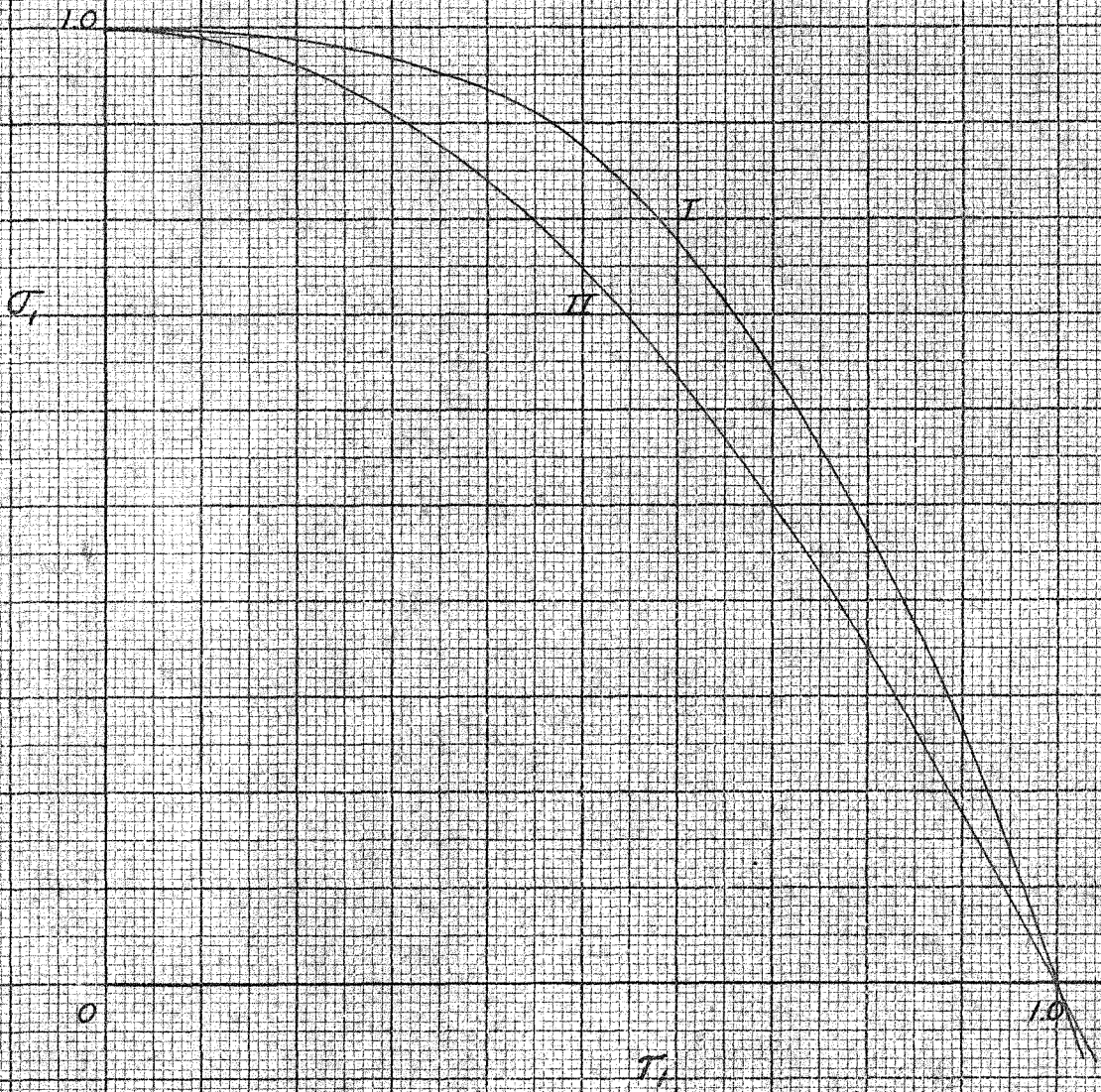


FIG. 6 $K\phi$ VS. ϕ EMPIRICAL

CURVE I $N=3$

CURVE II $N=2$

3

2

$K\phi$

1

0

10°

20°

30°

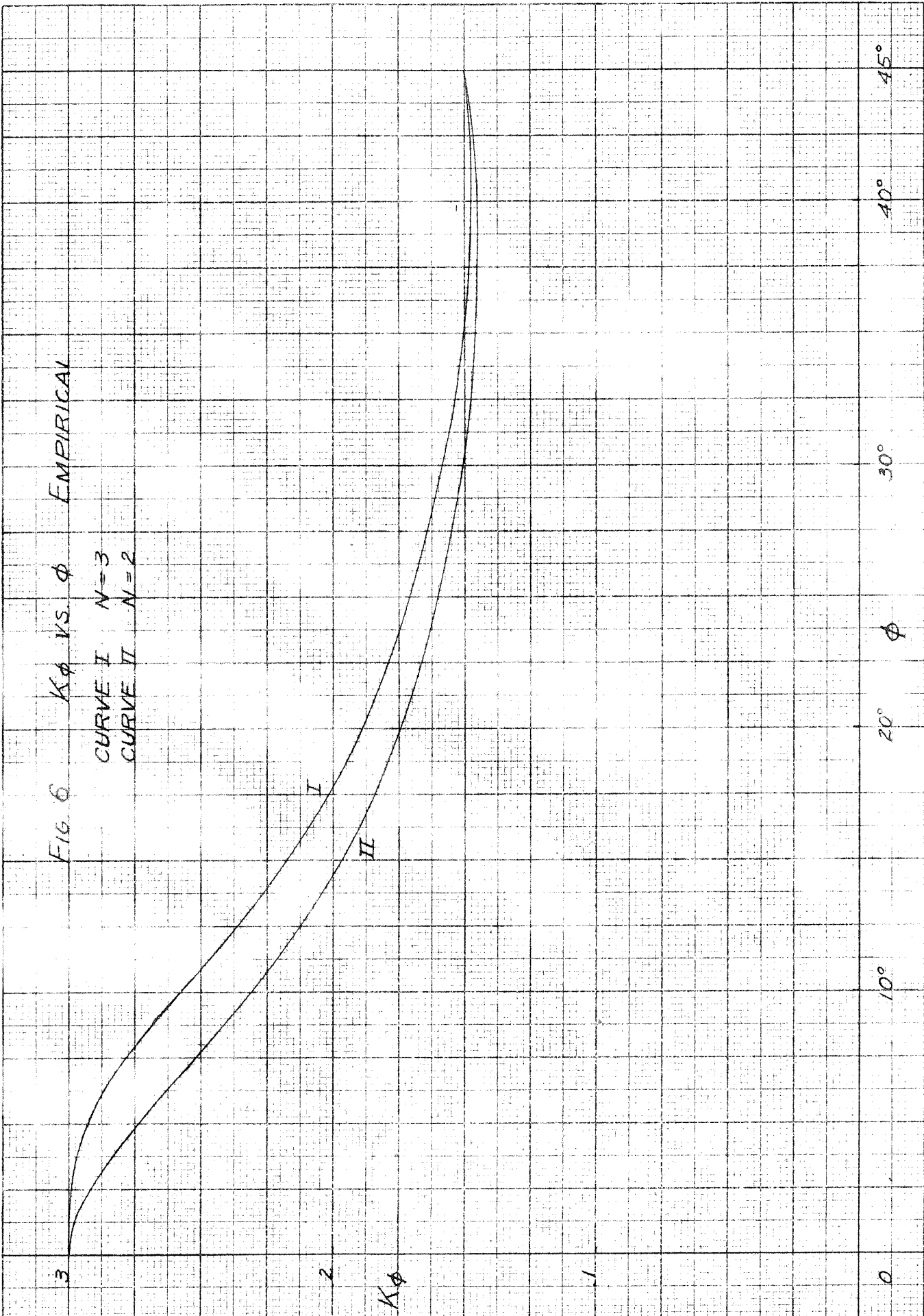
40°

45°

ϕ

I

II



V. THEORETICAL $K\phi$ CURVE:

The problem is now to explain the form of the $K\phi$ vs. ϕ curves of fig. 6. If this can be done, equation (1) will be justified and the chief aim of this thesis will be accomplished.

In equation (6):

$$\sigma\phi = K\phi \frac{Et}{R} \quad (6)$$

if the stress $\sigma\phi$ is a direct compression and R is the radius of the cylinder, then $K\phi = .3$ (constant). Obviously, in fig. 6, $K\phi$ is not a constant. Also obviously, the variation of $K\phi$ is caused by the fact that we are not dealing with simple compression parallel to the elements of a cylinder (except for $K\phi = .3$ at $\phi = 0$). Two important effects must be taken into account: curvature in the direction of $\sigma\phi$, and principal tension.

In order to calculate these effects, a major assumption must now be made. Assume that failure of the cylinder (for $\phi > 0$) occurs for finite deflections, rather than for stability. This is in agreement with Donnell's large deflection theory (ref. 3) and, in view of his remarks, seems to be the most probable type of failure.

A square element of sheet of length and width λ ($= \frac{1}{2}$ wave-length of buckled cylinder) will be considered as a curved column with the principal compression as end load and with

the normal component of principal tension as transverse load. Deflections can thus be calculated by means of ordinary engineering formulas. (Since length = λ , there is zero moment at the ends of the column).

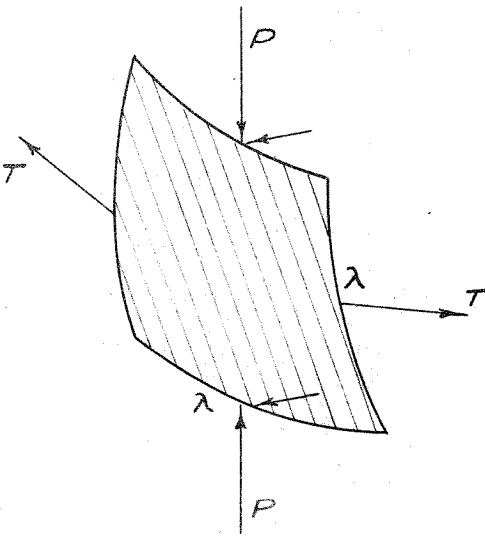


FIG. 7. FORCES ON SHEET ELEMENT

The deflection at the center of the square is:

$$y_0 = y_1 + y_2 \quad (16)$$

where y_1 = outward deflection of curved column under end load.

y_2 = inward deflection caused by inward component of tension.

Calculation of y_i :

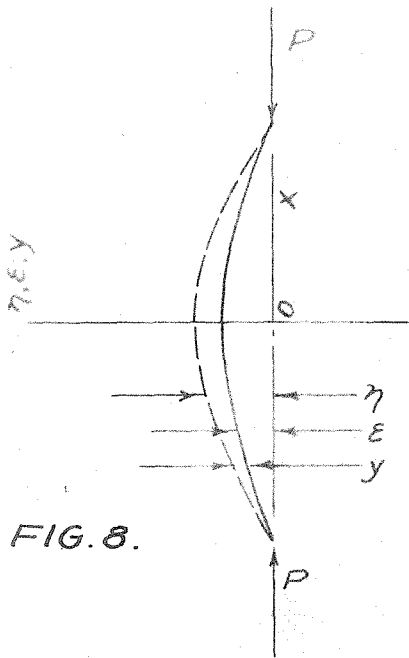


FIG. 8.

Let: y = elastic deflection

ϵ = initial displacement due to curve.

$$\eta = y + \epsilon$$

Approximately:

$$y = y_c \cos \frac{\pi x}{l}$$

Subscript (c) \curvearrowright center of column

$$\text{and } \epsilon = \epsilon_c \cos \frac{\pi x}{l}$$

$$\therefore \eta = (y_c + \epsilon_c) \cos \frac{\pi x}{l}$$

Equation of elastic bending:

$$\frac{d^2 y}{dx^2} = -\frac{P}{EI} (y_c + \epsilon_c) \cos \frac{\pi x}{l}$$

Integrating this, y is found:

$$y = \frac{P}{EI} (y_c + \epsilon_c) \frac{l^2}{\pi^2} \cos \frac{\pi x}{l}$$

(the constants of integration are zero for the axes in fig. 8).

$$\text{At } x = 0: \quad y = y_c = \frac{P}{EI} (y_c + \epsilon_c) \frac{l^2}{\pi^2}$$

$$\text{But } y_c = y_l$$

$$\frac{\pi^2 EI}{l^2} = P_0 = \text{Euler load}$$

$$P = P_\epsilon = \text{load on curved column}$$

$$\therefore y_i = \frac{\epsilon_c}{\frac{P_0}{P_\epsilon} - 1} \quad (17)$$

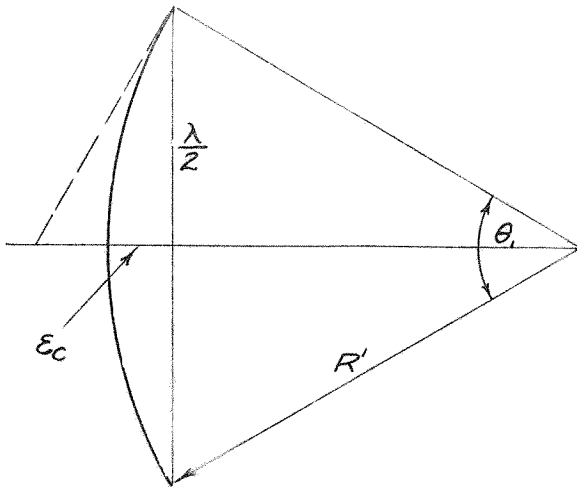


FIG. 9. RELATION OF ϵ_c TO λ AND R'

From fig. 9

$$\frac{\epsilon_c}{\frac{\lambda}{2}} = \frac{1}{2} \frac{\frac{\lambda}{2}}{R'}$$

$$\therefore \epsilon_c = \frac{\lambda^2 \sin^2 \phi}{8 r}$$

$$R' = \frac{r}{\sin^2 \phi}$$

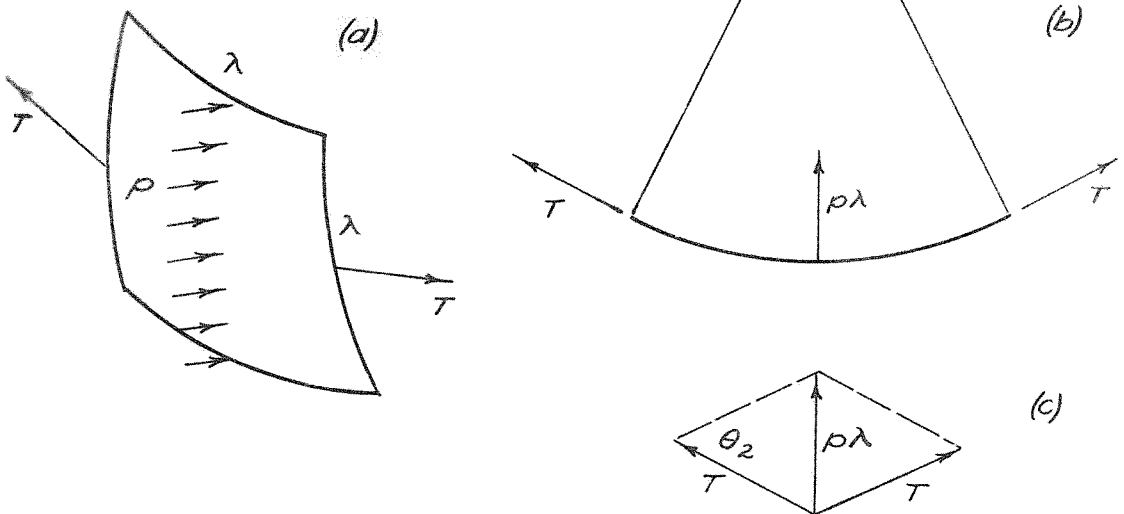
Finally, $\frac{E \epsilon}{P_0} = \frac{\text{load carried actually}}{\text{load for no eccentricity}} = \frac{K \phi}{.3}$

Substitute in equation (17):

$$\therefore y_1 = \frac{\lambda^2 \sin^2 \phi}{8 r \left(\frac{K \phi}{.3} - 1 \right)} \quad (18)$$

Calculation of y_2 :

FIG. 10.



Assume that the inward component of tension is evenly distributed along the length of the column (which is now considered as a beam).

$$p\lambda = T\theta_2 = \sigma_t + \lambda \cdot \frac{\lambda}{R}$$

$$\therefore p = \frac{\sigma_t + \lambda \cos^2 \phi}{r}$$

The amount of elastic support at the ends and along the edges is difficult to estimate. However, it seems reasonable to consider the element of sheet as a uniformly loaded beam with fixed ends.

The deflection for such a beam is:

$$y_2 = \frac{pl^4}{384 EI}$$

where $l = \lambda$

$$I = \frac{1}{12} \lambda t^3$$

$$y_2 = \frac{\sigma_t + \lambda \cos^2 \phi \lambda^4}{r \cdot 384 E \frac{1}{12} \lambda t^3}$$

But

$$\sigma_t = \sigma(\phi + 90^\circ)$$

$$= \sigma_\phi \tan \phi \left(\frac{\sin \phi - \tan 2\phi \cos \phi}{\cos \phi + \tan 2\phi \sin \phi} \right)$$

$$= -\sigma_\phi \tan^2 \phi$$

$$\sigma_\phi = K_\phi \frac{Et}{r} \cos^2 \phi$$

$$\therefore y_2 = -\frac{K_\phi \lambda^4}{32tr^2} \sin^2 \phi \cos^2 \phi$$

(19)

Note:

The outward component of compression is:

$$P_{\epsilon \theta_1} = \frac{\sigma_{\phi} + \lambda^2 \sin^2 \phi}{r}$$

$$\therefore p\lambda + P_{\epsilon \theta_1} = \frac{\sigma_{\phi} + \lambda^2 (\sin^2 \phi - \cos^2 \phi \tan^2 \phi)}{r} = 0$$

That is, the element of sheet is in equilibrium under the assumptions that have been made.

To return to the main discussion: the total deflection of the sheet is found by substituting equations (18) and (19) in equation (16).

$$y_0 = y_1 + y_2$$

$$= \frac{\lambda^2 \sin^2 \phi}{8r \left(\frac{.3}{K\phi} - 1 \right)} - \frac{K\phi \lambda^4 \sin^2 \phi \cos^2 \phi}{32tr^2} \quad (20)$$

Equation (20) gives the deflection in terms of $K\phi$, ϕ and the properties of the cylinder. It is now necessary to find a criterion for failure, i.e. an allowable value for y_0 .

The assumption has already been made that failure occurs for finite deflections. This means that at failure the yield point of the material is reached locally and in order to find y_0 , it is necessary to calculate the maximum local stress.

For the curved column:

$$\begin{aligned} \sigma_{max.} &= \frac{P}{A} + \frac{Mc}{I} \\ &= \sigma_{\phi} + \frac{\sigma_{\phi} + \lambda (y_0 + \epsilon) \frac{t}{2}}{\frac{1}{12} \lambda t^3} \end{aligned}$$

$$\begin{aligned}\sigma_{max} &= \sigma_{\phi} \left[1 + \frac{6(y_0 + \epsilon)}{t} \right] \\ &= K_{\phi} \frac{Et}{r} \cos^2 \phi \left[1 + \frac{6(y_0 + \frac{\lambda^2}{8r} \sin^2 \phi)}{t} \right]\end{aligned}$$

But $\sigma_{max} = Y = \text{const.}$

$$\therefore y_0 = \frac{Yr}{6K_{\phi} E \cos^2 \phi} - \frac{t}{6} - \frac{\lambda^2}{8r} \sin^2 \phi \quad (21)$$

Eliminate y_0 from equations (20) and (21).

$$\begin{aligned}\therefore \frac{\lambda^2 \sin^2 \phi}{8rt \left(\frac{3}{K_{\phi}} - 1 \right)} - \frac{K_{\phi} \lambda^4 \sin^2 \phi \cos^2 \phi}{32r^2 t^2} \\ = \frac{Yr}{6Et K_{\phi} \cos^2 \phi} - \frac{1}{6} - \frac{\lambda^2 \sin^2 \phi}{8rt}\end{aligned} \quad (22)$$

This is an equation between K_{ϕ} and ϕ . It involves the two parameters $\frac{Yr}{Et}$ and $\frac{\lambda^2}{rt}$. The first of these is obviously a constant, since it involves only the physical properties and dimensions of the sheet.

The latter parameter, $\frac{\lambda^2}{rt}$, is assumed to be independent of ϕ . Experimentally, λ has been observed to be constant (or nearly so) for a given series of cylinders. Since r and t are both constant, the fraction $\frac{\lambda^2}{rt}$ is approximately constant.

In order to determine the form of equation (22), definite values will be given to the physical parameters and a curve will

be plotted.

$$\text{Let: } \frac{\lambda^2}{rt} = 12 \quad \frac{r}{t} = 300 \quad \left(\frac{\lambda}{r} = \frac{1}{5} \right)$$

$$Y = 4 \times 10^4 \quad E = 2 \times 10^7$$

Substitute these values in equation (22):

$$\frac{1.5 \sin^2 \phi}{\left(\frac{.3}{K\phi} - 1 \right)} - 4.5 \sin^2 \phi \cos^2 \phi K\phi = \frac{.1}{K\phi \cos^2 \phi} - \frac{1}{6} - 1.5 \sin^2 \phi \quad (23)$$

It is possible to solve this equation explicitly for $K\phi$. A much quicker and easier method is to assign values to ϕ and find $K\phi$ by trial and error. The table below is the result.

| | | | | | | |
|---------|--------|-----|-----|------|------|------|
| ϕ | = 10 | 20 | 30 | 40 | 45 | 60 |
| $K\phi$ | = .251 | .20 | .16 | .142 | .142 | .162 |

The value for $\phi = 60^\circ$ was computed in order to make certain that the curve has a minimum near $\phi = 45^\circ$ (a feature of the experimental curves).

The theoretical $K\phi$ vs. ϕ curve is shown in fig. 11.

Trial calculations have shown that practically the same curve results if we take:

$$\frac{\lambda^2}{rt} = 19 \quad \frac{r}{t} = 300 \quad \frac{Y}{E} = \frac{1}{400}$$

That is, a 50% change of $\frac{\lambda^2}{rt}$ has the same effect as a 20% change of $\frac{Y}{E} \frac{r}{t}$. Furthermore, the variation of $\frac{Y}{E} \frac{r}{t}$ from one series to another is much larger than that of $\frac{\lambda^2}{rt}$. Thus it is easy to see that the quantity $\frac{Y}{E} \frac{r}{t}$ is of greatest importance in equation (22), and should therefore, be a vital factor in the value of the component n.

Agreement between the theoretical curve and the experimental curve (shown dotted in fig. 11) is very good; and indicates that the explanation and theory that have been given are approximately correct. The coordination of theory and experiment can be carried a little farther, but it is first necessary to give the experimental data.

For clarity, the important assumptions are repeated here.

1) Buckling takes place in the direction of principal compression.

2) In pure compression:

$$\sigma_{\phi} = .3 \frac{Et}{r}$$

In pure torsion

$$\sigma_{\phi} = .15 \frac{Et}{r}$$

3) Failure is for finite deflections, yield stress.

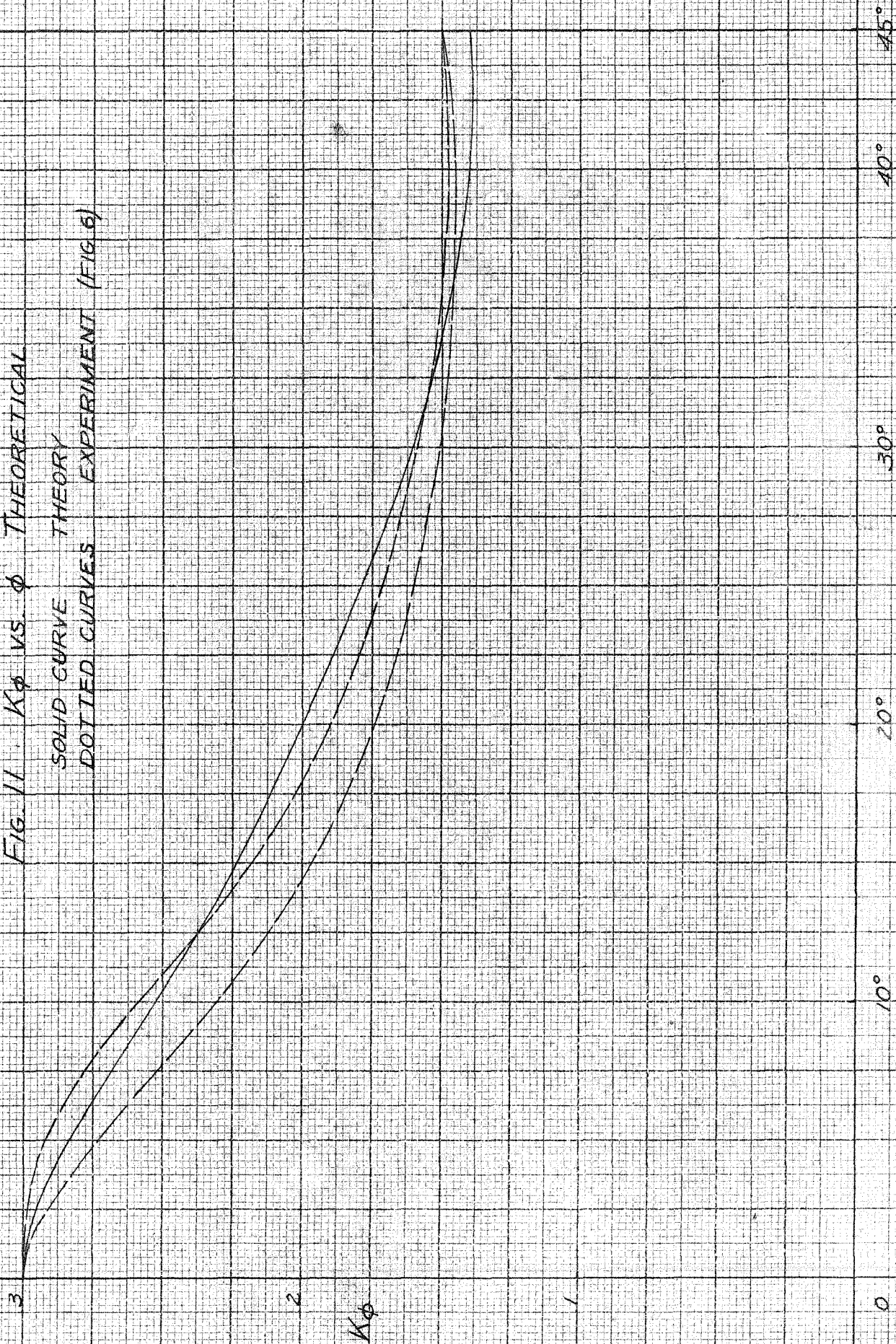
4) Deflections can be calculated separately and added.

5) $\frac{\lambda^2}{rt} = \text{const.}$ for a given series of cylinders:

i.e. $\frac{\lambda^2}{rt}$ is independent of ϕ .

Assumptions (2) and (5) are theoretically not necessary to solve the problem. However, they both are based on observation and result in an immense simplification of the analysis.

FIG. 11. $K\phi$ VS. ϕ THEORETICAL
SOLID CURVE THEORY
DOTTED CURVES EXPERIMENT (FIG. 6)



VI. EXPERIMENTAL RESULTS:

Tests were performed by means of a compression-torsion-bending machine that Dr. Donnell designed and built several years ago. A complete description of the machine and the technique of its use is given in Donnell's report on pure torsion (ref. 2). A few very small changes have since been made; but on the whole, the method of testing has not altered appreciably, so that a repetition of the procedure need not be included here.

Cylinders tested were all of circular cross-section, 6 inches in length and about 1-7/8 inches in diameter. The effect of variable $\frac{1}{d}$ is disregarded, except in one or two of Bridget's tests. Wall thicknesses varied from .002 in. to .010 in., and materials included spring copper, soft copper, spring brass, soft brass, steel and zinc. In this way a very large range of physical properties has been covered.

Results are quite simple. In every case a curve of the type

$$1 - \frac{\sigma}{\sigma_0} = \left(\frac{\tau}{\tau_0} \right)^n$$

occurs. The value of n is, of course, determined graphically.

Two simple methods are available for doing this. (1) Bridget's method was to plot the points on logarithmic paper and measure the slope of the resulting straight line. (2) The method used here is to measure the slope of the $\frac{\sigma}{\sigma_0}$ vs. $\frac{\tau}{\tau_0}$ curve (in ordinary

coordinates) near $\frac{\tau}{\tau_0} = 1$.

Differentiate equation (1)

$$d\left(1 - \frac{\sigma}{\sigma_0}\right) = n \left(\frac{\tau}{\tau_0}\right)^{n-1} d\left(\frac{\tau}{\tau_0}\right)$$

$$-\frac{d\left(\frac{\sigma}{\sigma_0}\right)}{d\left(\frac{\tau}{\tau_0}\right)} = n \left(\frac{\tau}{\tau_0}\right)^{n-1}$$

∴ At $\frac{\tau}{\tau_0} = 1$

$$\text{Slope} = \frac{d\sigma_i}{d\tau_i} = -n$$

This has been necessary because in some cases the testing machine was not strong enough to break the specimens in pure compression and a larger compression machine had to be used. Many of the present series of tests have intermediate points only on the lower parts of the curves for that reason.

A summary of the useful data is given below. Letters refer to Bridget's tests, numbers refer to tests made by the author. Curves and detailed data are placed at the end of the thesis.

| No. | n | Mat'l. | t | Di. | l | $\frac{E_{tens}}{x 10^{-7}}$ | $\frac{Y_{tens}}{x 10^{-3}}$ | $\frac{\sigma_r}{E_t}$ | $\frac{\tau_r}{E_t}$ | No. |
|-----|-----|----------|-------|------|-------|------------------------------|------------------------------|------------------------|----------------------|------|
| (1) | (2) | (3) | (4) | (5) | (6) | (7) | (8) | (9) | (10) | (11) |
| 1 | 2.4 | Spr. Cu. | .0104 | 1.88 | 5.7 | 1.67 | 24 | .25 | .098 | .13 |
| 2 | 2.3 | " | .0084 | " | " | 1.66 | 27 | .33 | .099 | .18 |
| 3 | 2.2 | " | .0066 | " | " | 1.76 | 35 | .31 | .087 | .20 |
| 4 | 2.1 | " | .0055 | " | " | 1.67 | 28 | .31 | .085 | .26 |
| 5 | 5.5 | So. Cu. | .0068 | " | " | 1.45 | 4.6 | .09 | .047 | .04 |
| 6 | --- | Steel | .0104 | " | " | 3.13 | 43 | .23 | .088 | .12 |
| 7 | 3.1 | " | .0063 | " | " | 3.26 | 49 | .36 | .082 | .22 |
| 8 | 2.5 | " | .0054 | " | " | 3.12 | 48 | .30 | .080 | .27 |
| 9 | 4.1 | Spr. Br. | .0066 | " | " | 1.69 | 31 | .36 | .088 | .26 |
| 10 | 2.5 | So. Br. | .0053 | " | " | 1.39 | 5.3 | .20 | .061 | .07 |
| 11 | 5.0 | So. Cu. | .0113 | " | " | 1.55 | 4.6 | .05 | .026 | .03 |
| 12 | 3.0 | Zinc | .0062 | " | " | .78 | 3.7 | .17 | .088 | .07 |
| A | 1.8 | Steel | .0020 | 1.88 | 5.32 | 3.14 | 58 | .28 | .075 | .88 |
| B | 3.3 | Spr. Br. | .0032 | " | " | 1.65 | 27 | .24 | .073 | .48 |
| C | 2.1 | Steel | .0030 | 3.75 | " | 3.06 | 49 | .17 | .073 | 1.00 |
| D | 2.7 | " | .0020 | 1.88 | 11.32 | 2.71 | 58 | .23 | .055 | 1.02 |
| E | 2.3 | " | .0030 | " | 5.32 | 3.06 | 49 | .29 | .066 | .50 |
| F | 2.2 | " | .0020 | 3.75 | 1.32 | 3.14 | 58 | .17 | .108 | 1.68 |
| G | 3.0 | " | .0040 | 1.88 | 5.32 | 2.96 | 36 | .20 | .064 | .28 |

1
No
1

The average value of \underline{n} is 2.7, a value which is not very useful for design because of the amount of scatter. Variations in \underline{n} are discussed in section VII below.

Averages of column (9) and (10) are .25 and .075 respectively, and agree reasonably well with the assumptions .3 and .075 in the theory. A few very low values of these coefficients occur for materials with extremely low yield points. As has been discussed by other experimenters (ref. 5), soft- or thick-walled cylinders do not fail in quite the same manner as do thin-walled cylinders that are made of hard materials. Since the latter is the important type structurally, the low values mentioned above do not seriously affect the discussion.

VII. COORDINATION OF THEORY WITH EXPERIMENT:

As has already been mentioned, the curve of $K\phi$ vs. ϕ as found by analysis, agrees with the empirical curve. Also, the theoretical curve has been shown to depend largely upon the parameter $\frac{Y}{E} \frac{r}{t}$. A plot of experimental values of \underline{n} against this quantity gives interesting results; The points all lie within a sharply defined region (see figure 12). Causes of variation within that region have not yet been found. Perhaps anisotropy of the material is an important factor in the value of \underline{n} ; or perhaps an inaccuracy of the assumption that $\frac{\lambda^2}{rt}$ is independent of ϕ is the cause of the trouble. Future, more exhaustive experiments will be necessary to determine the answer to this question.

For the present, it is recommended that the "median" curve be used for design. The method is as follows:

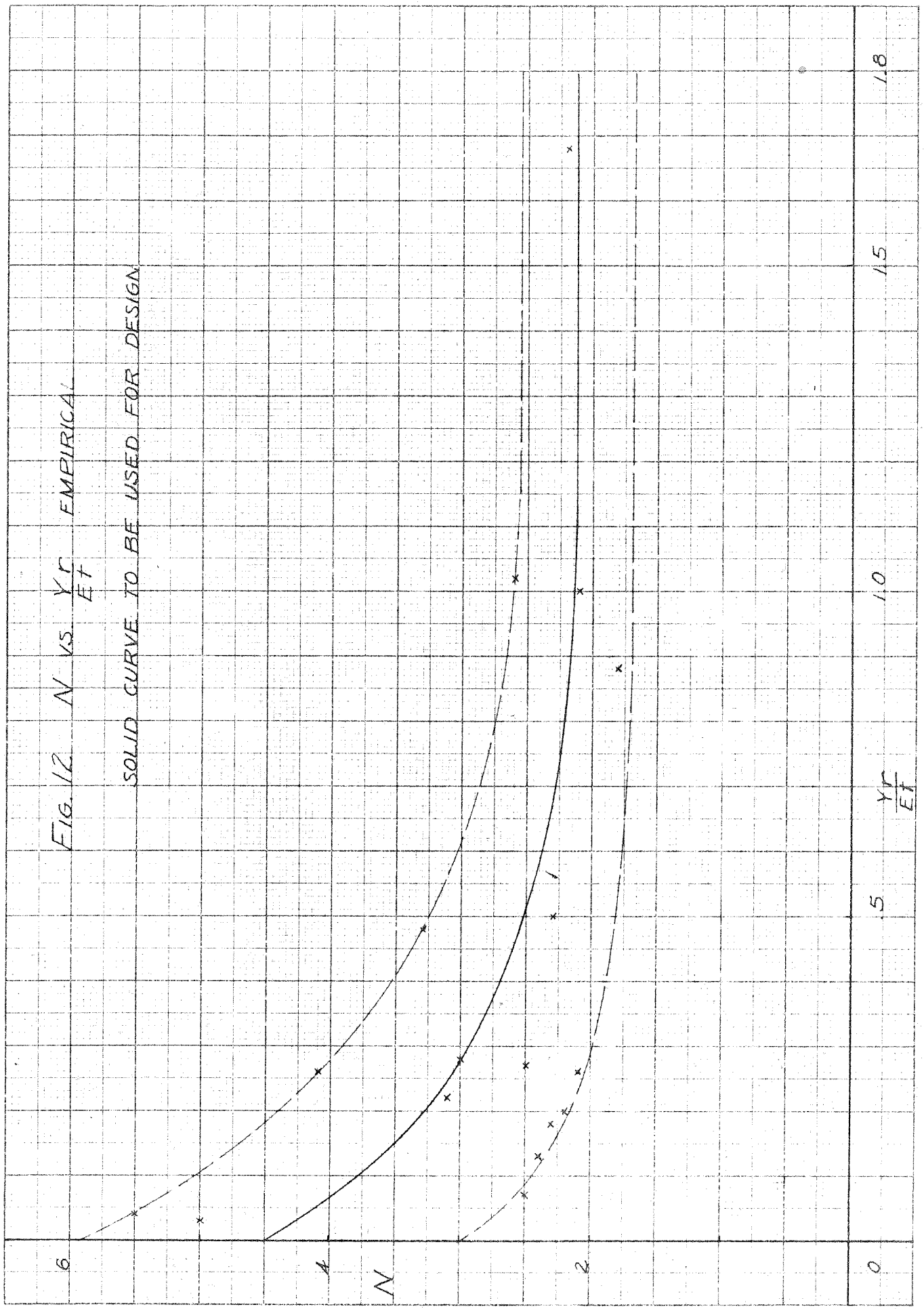
- 1) From the properties of the material and dimensions of the cylinder, calculate $\frac{Y}{E} \frac{r}{t}$.
- 2) Use figure 12 to find the value of exponent \underline{n} (middle curve).
- 3) Calculate σ_0 and τ_0 from formulas (7) and (8).
- 4) Interpolate or extrapolate the curves of figure 5 to get the curve which corresponds to the value of \underline{n} found above.

5) From the curve found in 4) above find $\frac{\sigma}{\sigma_0}$ for a given $\frac{\tau}{\tau_0}$ or vice versa.

One more point deserves mention. Equation (22) depends for its form upon the values of $\frac{\lambda^2}{rt}$ and $\frac{Y}{E} \frac{r}{t}$. These are both independent of units or actual size of the cylinder. Hence, the value of n has no scale effect, and results of model experiments can be used directly for large scale work.

FIG. 12 N vs $\frac{Y_r}{E_T}$ EMPIRICAL

SOLID CURVE TO BE USED FOR DESIGN



VIII. ACKNOWLEDGMENT:

The author of this thesis is very grateful indeed for the large amount of help that has come from the GALCIT staff during the performance of the experiments and development of the theory. Without the assistance of Drs. von Karman, C. E. Millikan, A. L. Klein, and E. E. Sechler this paper could not have been written.

I wish also thank Dr. Donnell and Lieutenant Bridget for instruction in testing technique during the first part of the experimental work.

References

1. Bridget New Experiments on Thin Walled Structures.
 A.S.M.E. Trans. Vol. 56, August 1934.
2. Donnell Stability of Thin Walled Tubes under Torsion.
 N.A.C.A. Rep. 479.
3. Donnell New Theory for Buckling of Cylinders.
 A.S.M.E. Trans. Vol. 56, No. 11, Nov., 1934.
4. Mossman Bending of Metal Monocoque Construction.
 Robinson T.N. 557.
5. Lundquist Compression Tests of Thin Walled Cylinders.
 N.A.C.A. Rep. 475.

Notation

| | |
|--------------------|---|
| σ_y, σ | Unit compressive stress applied parallel to elements of cylinder (all stresses in force per unit area). |
| τ | Unit shear stress due to torsion. |
| ϕ | Angle between principal compression and elements of cylinder. |
| σ_ϕ | Principal compressive stress. |
| σ_t | Principal tensile stress |
| d | Diameter of cylinder |
| r | Radius |
| t | Thickness of wall |
| R | Radius of curvature in direction of σ_t |
| R' | Radius in direction of σ_ϕ |
| σ_0 | Failure compressive stress for $\phi = 0$ (pure compression) |
| τ_0 | Failure shear stress for pure torsion |
| $K\phi$ | "Relative strength" = $\frac{\sigma_\phi R}{Et}$ |
| E | Young's Modulus |
| Y | Yield stress |
| λ | Half wave length of buckled sheet |
| $P = P_\epsilon$ | Resultant of compressive forces along edge of square element |
| T | Resultant of tensile forces along edge of element |
| p | Uniformly distributed load due to tension (force/unit length) |

Notation (cont'd)

| | | |
|------------|----------------------|--|
| y_0 | | Deflection of sheet at failure |
| y_1 | | Deflection due to compression |
| y_2 | | Deflection due to tension |
| θ_1 | $\frac{\lambda}{R'}$ | Angle between opposed compressive forces |
| θ_2 | $\frac{\lambda}{R}$ | Angle between opposed tensile forces |
| l | | Length of cylinder |

Experimental Data

C = pounds compression

T = inch pounds torsion

$$\therefore \frac{C}{C_0} = \frac{\sigma}{\sigma_0}, \quad \frac{T}{T_0} = \frac{\tau}{\tau_0}$$

Test No. 1

| | | | | | | |
|-----|------|------|-----|-----|------|------|
| C = | 0 | 0 | 500 | 500 | 2560 | 2640 |
| T = | 1034 | 1052 | 954 | 968 | 0 | 0 |

Test No. 2

| | | | | | | |
|-----|-----|-----|-----|-----|-----|-----|
| C = | 0 | 0 | 0 | 200 | 300 | 200 |
| T = | 682 | 694 | 698 | 680 | 656 | 662 |

| | | | | | | |
|-----|-----|-----|-----|-----|-----|-----|
| C = | 500 | 500 | 600 | 600 | 700 | 700 |
| T = | 618 | 650 | 598 | 624 | 580 | 616 |

| | | | | | | |
|-----|------|------|--|--|--|--|
| C = | 2420 | 2500 | | | | |
| T = | 0 | 0 | | | | |

Test No. 3

| | | | | | | |
|-----|-----|-----|-----|-----|-----|-----|
| C = | 0 | 0 | 200 | 400 | 500 | 600 |
| T = | 390 | 390 | 366 | 342 | 330 | 320 |

| | | | | | | |
|-----|-----|------|------|--|--|--|
| C = | 600 | 1490 | 1520 | | | |
| T = | 318 | 0 | 0 | | | |

Experimental Data (cont'd)

Test No. 4

| | | | | | | |
|-----|-----|-----|-----|-----|-----|-----|
| C = | 0 | 0 | 100 | 100 | 200 | 300 |
| T = | 252 | 256 | 224 | 248 | 224 | 212 |
| C = | 300 | 400 | 400 | 980 | 980 | |
| T = | 212 | 202 | 208 | 0 | 0 | |

Test No. 5

| | | | | | | |
|-----|-----|-----|-----|-----|-----|-----|
| C = | 0 | 0 | 50 | 100 | 100 | 150 |
| T = | 186 | 188 | 180 | 180 | 184 | 172 |
| C = | 200 | 360 | 380 | 380 | | |
| T = | 168 | 0 | 0 | 0 | | |

Test No. 6. Discarded. Too strong for testing machine.

Test No. 7

| | | | | | | |
|-----|------|------|------|-----|-----|-----|
| C = | 0 | 0 | 200 | 400 | 400 | 600 |
| T = | 630 | 624 | 616 | 608 | 614 | 578 |
| C = | 3030 | 2890 | 2930 | | | |
| T = | 0 | 0 | 0 | | | |

Test No. 8

| | | | | | | | |
|-----|-----|-----|-----|-----|-----|------|------|
| C = | 0 | 0 | 200 | 500 | 500 | 1790 | 1730 |
| T = | 424 | 442 | 404 | 374 | 388 | 0 | 0 |

Experimental Data (cont'd)

Test No. 9

| | | | | | | | |
|-----|-----|-----|-----|-----|-----|------|------|
| C = | 0 | 0 | 0 | 0 | 200 | 200 | 300 |
| T = | 376 | 392 | 376 | 378 | 348 | 378 | 374 |
| C = | 400 | 400 | 500 | 500 | 500 | 1630 | 1650 |
| T = | 368 | 350 | 362 | 344 | 346 | 0 | 0 |

Test No. 10

| | | | | | | | |
|-----|-----|-----|-----|-----|-----|-----|-----|
| C = | 0 | 0 | 100 | 200 | 200 | 500 | 498 |
| T = | 144 | 138 | 130 | 118 | 118 | 0 | 0 |

Test No. 11

| | | | | | | | |
|-----|-----|-----|-----|-----|-----|-----|-----|
| C = | 0 | 0 | 0 | 0 | 300 | 300 | 400 |
| T = | 300 | 286 | 300 | 292 | 270 | 270 | 256 |
| C = | 593 | 597 | 595 | | | | |
| T = | 0 | 0 | 0 | | | | |

Test No. 12

| | | | | | | | |
|-----|-----|-----|-----|-----|-----|-----|-----|
| C = | 0 | 0 | 0 | 0 | 100 | 100 | 150 |
| T = | 182 | 160 | 164 | 158 | 150 | 146 | 122 |
| C = | 305 | 314 | 322 | | | | |
| T = | 0 | 0 | 0 | | | | |

Experimental Data (cont'd)

Test No. A

| | | | | | | | |
|-----|-----|-----|-----|-----|-----|-----|-----|
| C = | 0 | 20 | 40 | 60 | 80 | 100 | 120 |
| T = | 56 | 52 | 49 | 47 | 40 | 39 | 36 |
| C = | 170 | 172 | 230 | 213 | 231 | | |
| T = | 30 | 20 | 10 | 0 | 0 | | |

Test No. B

| | | | | | | | |
|-----|----|-----|-----|-----|-----|-----|-----|
| C = | 20 | 110 | 150 | 175 | 190 | 230 | 250 |
| T = | 70 | 64 | 60 | 56 | 54 | 30 | 0 |

Test No. C

| | | | | | | | |
|-----|-----|-----|-----|-----|-----|-----|-----|
| C = | 0 | 50 | 150 | 155 | 200 | 220 | 230 |
| T = | 240 | 226 | 180 | 174 | 123 | 93 | 70 |
| C = | 250 | 279 | 237 | 237 | | | |
| T = | 100 | 72 | 0 | 0 | | | |

Test No. D

| | | | | | | | |
|-----|----|----|-----|-----|-----|--|--|
| C = | 0 | 40 | 120 | 150 | 151 | | |
| T = | 36 | 34 | 24 | 11 | 10 | | |

Test No. E

| | | | | | | | |
|-----|-----|-----|-----|-----|-----|-----|-----|
| C = | 0 | 0 | 100 | 100 | 200 | 300 | 300 |
| T = | 106 | 110 | 96 | 100 | 90 | 64 | 63 |
| C = | 490 | 520 | | | | | |
| T = | 0 | 0 | | | | | |

Experimental Data (cont'd)

Test No. F

| | | | | | |
|-----|-----|-----|-----|-----|-----|
| C = | 0 | 25 | 75 | 100 | 132 |
| T = | 160 | 170 | 130 | 96 | 0 |

Test No. G

| | | | | | | | |
|-----|-----|-----|-----|-----|-----|-----|-----|
| C = | 0 | 0 | 0 | 0 | 100 | 100 | 200 |
| T = | 178 | 196 | 186 | 184 | 172 | 180 | 166 |

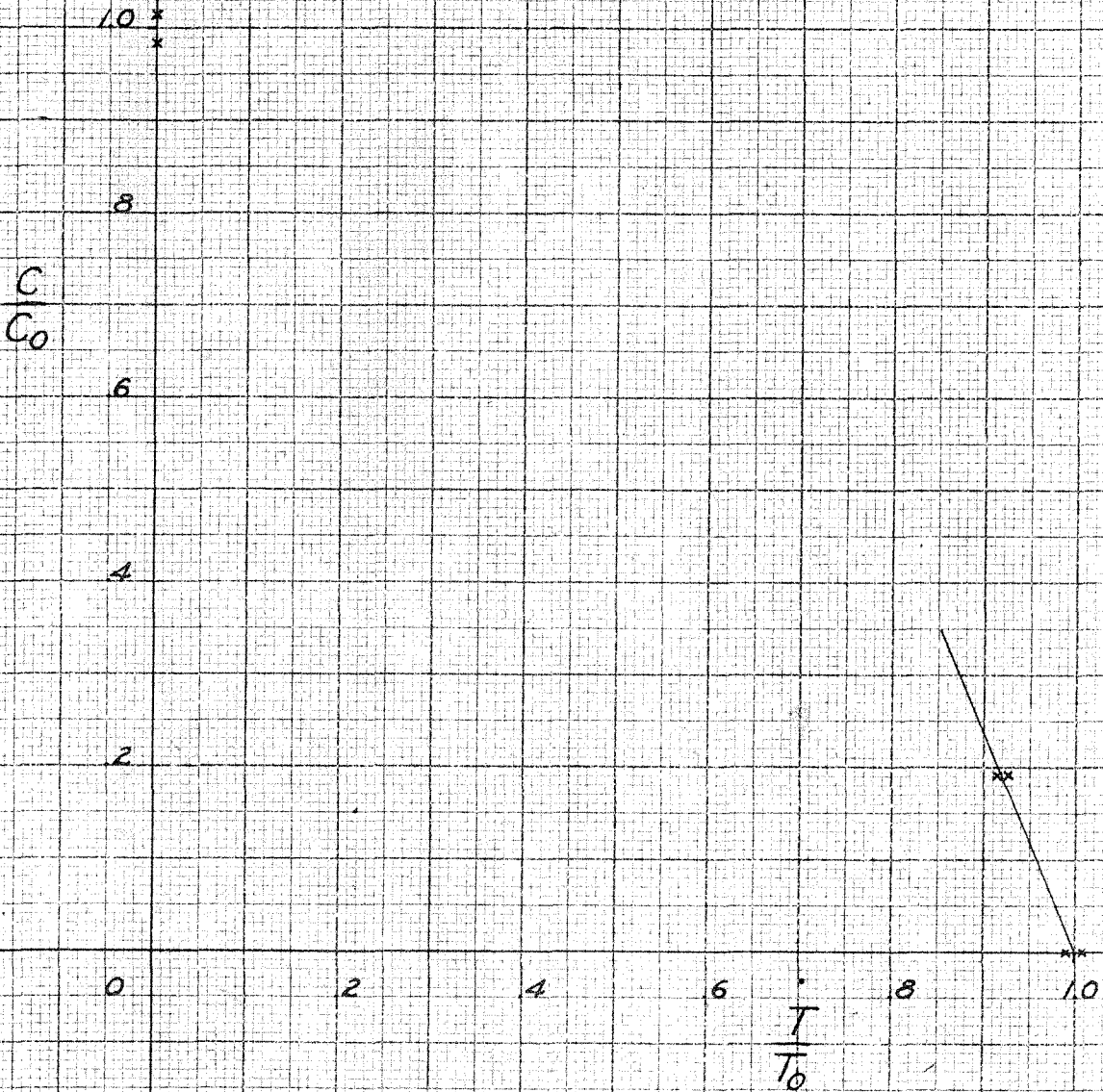
| | | | | | | | |
|-----|-----|-----|-----|-----|-----|-----|-----|
| C = | 200 | 300 | 380 | 400 | 500 | 500 | 500 |
| T = | 174 | 144 | 150 | 124 | 0 | 75 | 132 |

| | | | | | | |
|-----|-----|-----|-----|-----|-----|-----|
| C = | 500 | 540 | 595 | 613 | 610 | 660 |
| T = | 140 | 100 | 60 | 0 | 0 | 0 |

COMPRESSION VS. TORSION

TEST NO. 1. SPRING COPPER

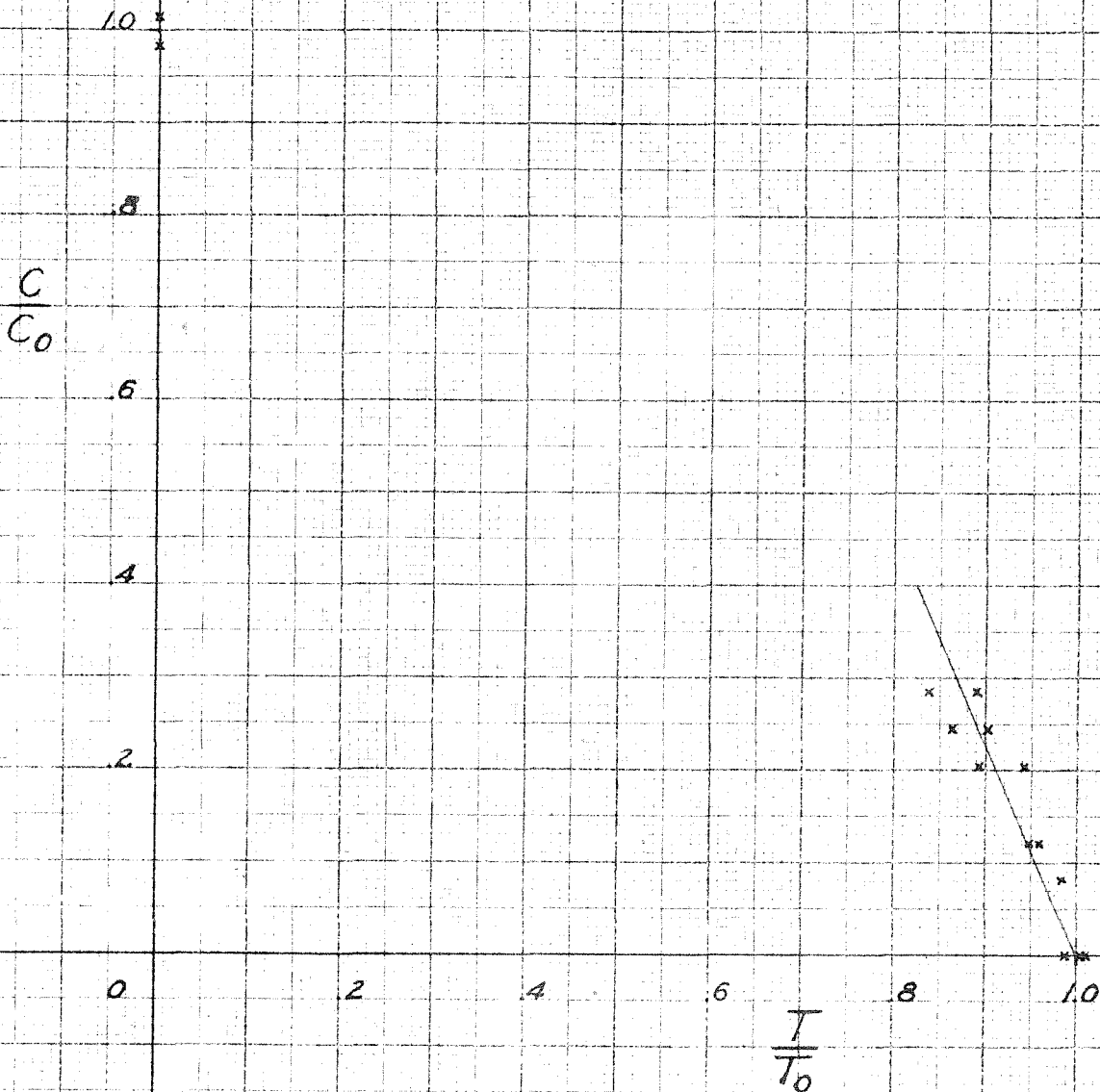
$T = .0104$ IN. $N = 2.4$



COMPRESSION VS. TORSION

TEST NO. 2 SPRING COPPER

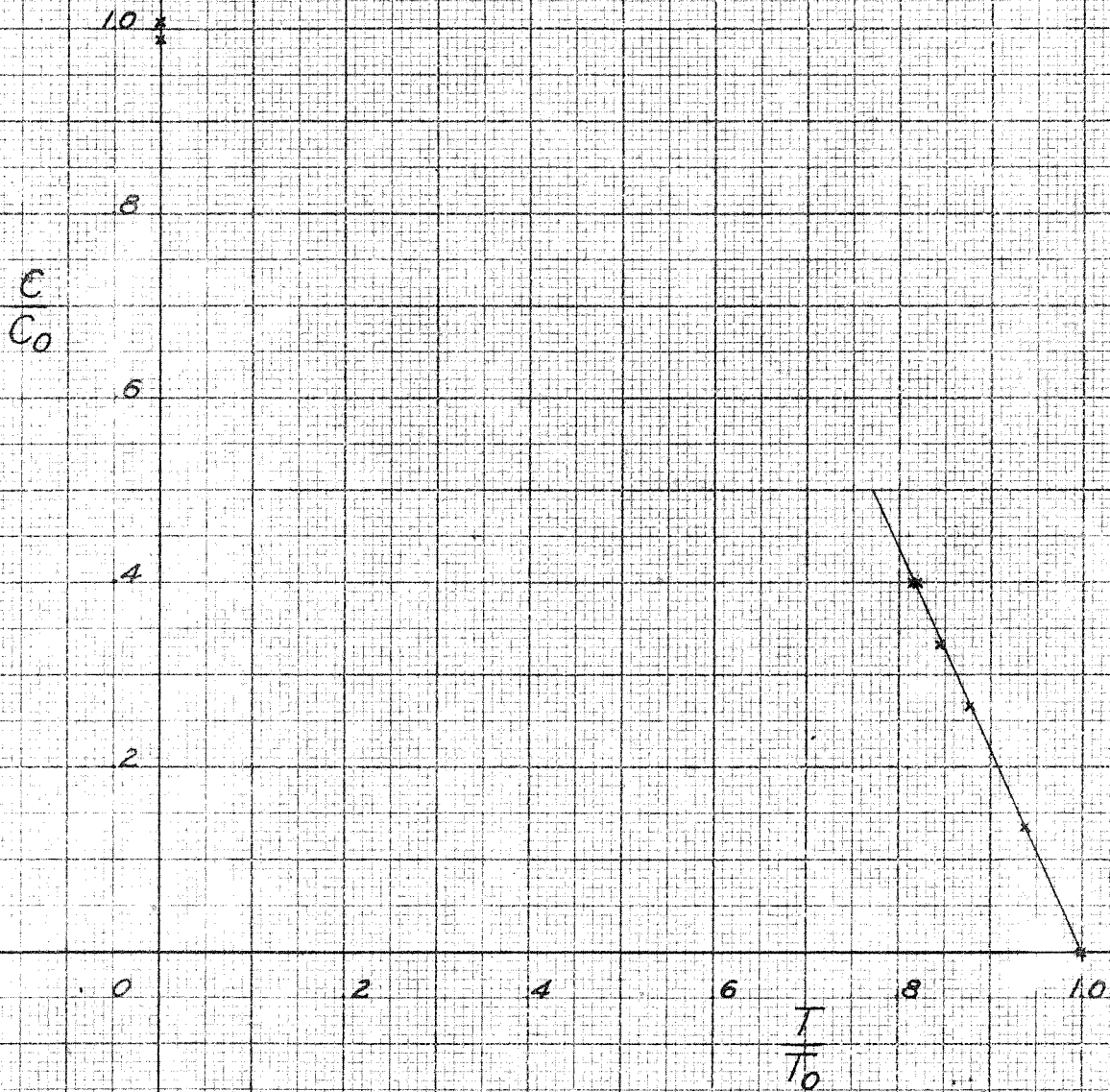
$T = .0084$ $N = 2.3$



COMPRESSION VS. TORSION

TEST NO. 3. SPRING COPPER

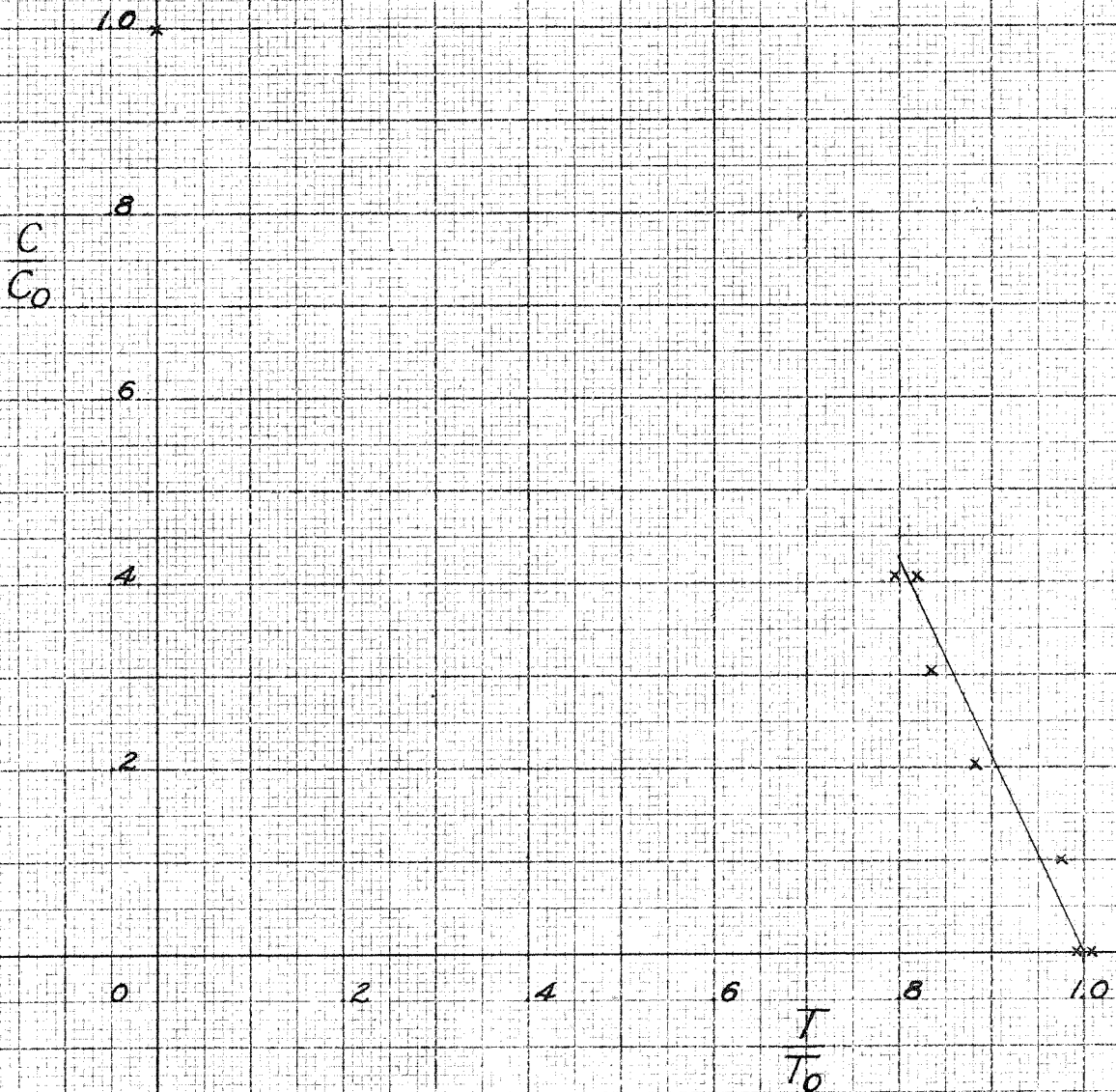
$T = .0066$ $N = 2.2$



COMPRESSION VS TORSION

TEST NO. 4. SPRING COPPER

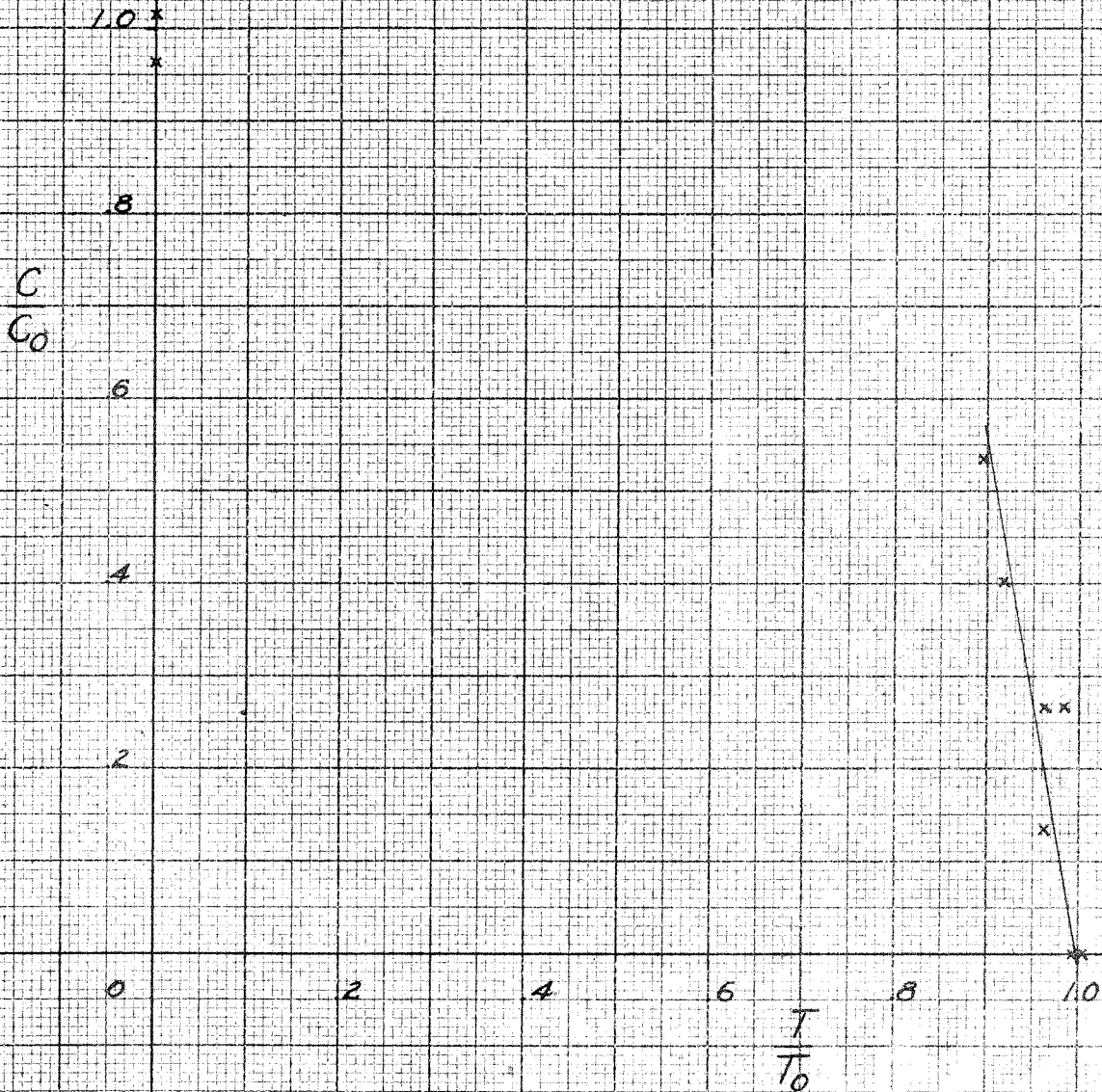
$T = .0055$ $N = 2.1$



COMPRESSION VS. TORSION

TEST NO. 5. SOFT COPPER

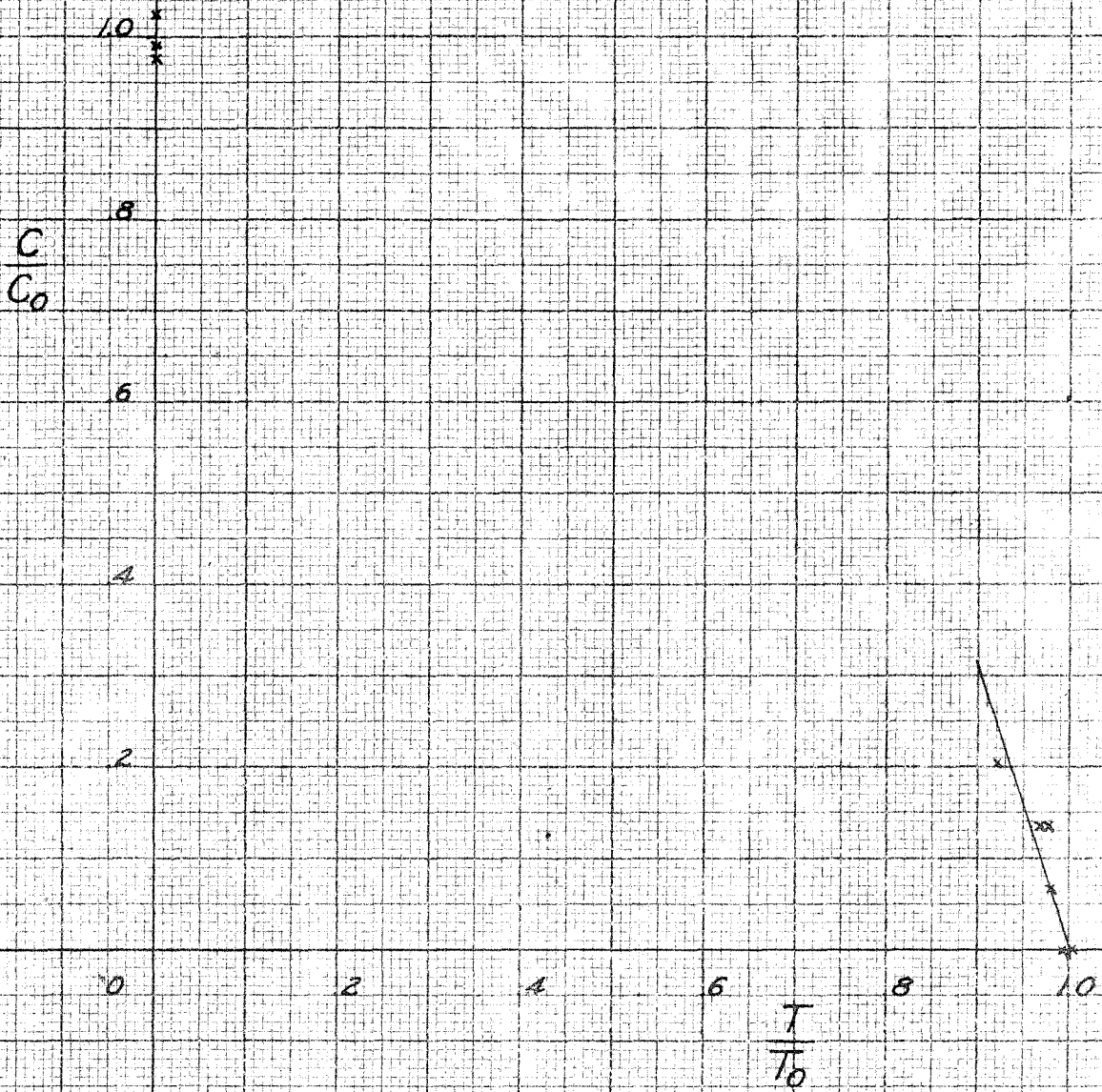
$T = .0068$ $N = 5.5$



COMPRESSION VS TORSION

TEST NO. 7 STEEL

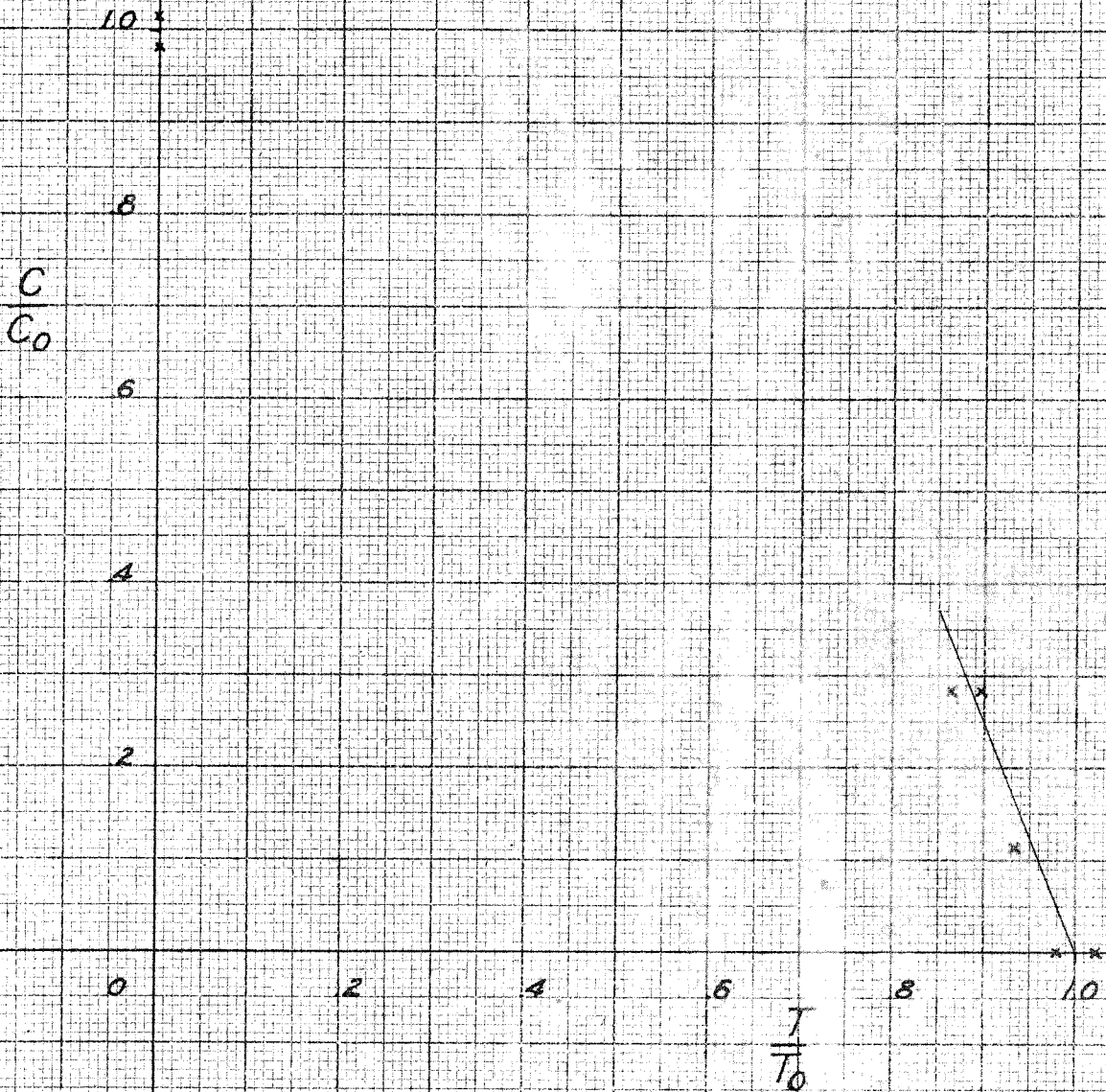
$T = .0063$ $N = 3.1$



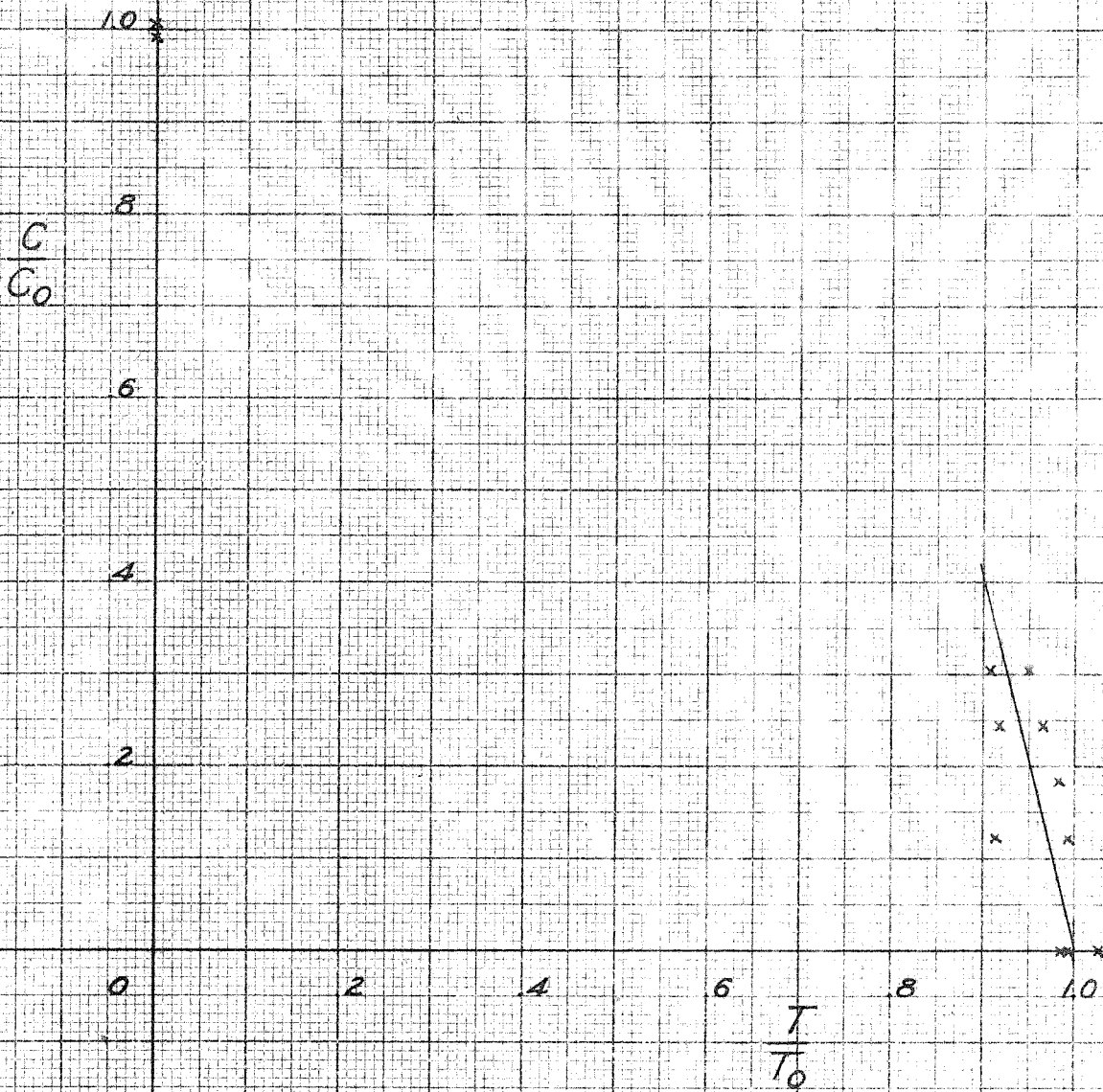
COMPRESSION VS. TORSION

TEST NO. 8. STEEL

$T = .0054$ $N = 2.5$



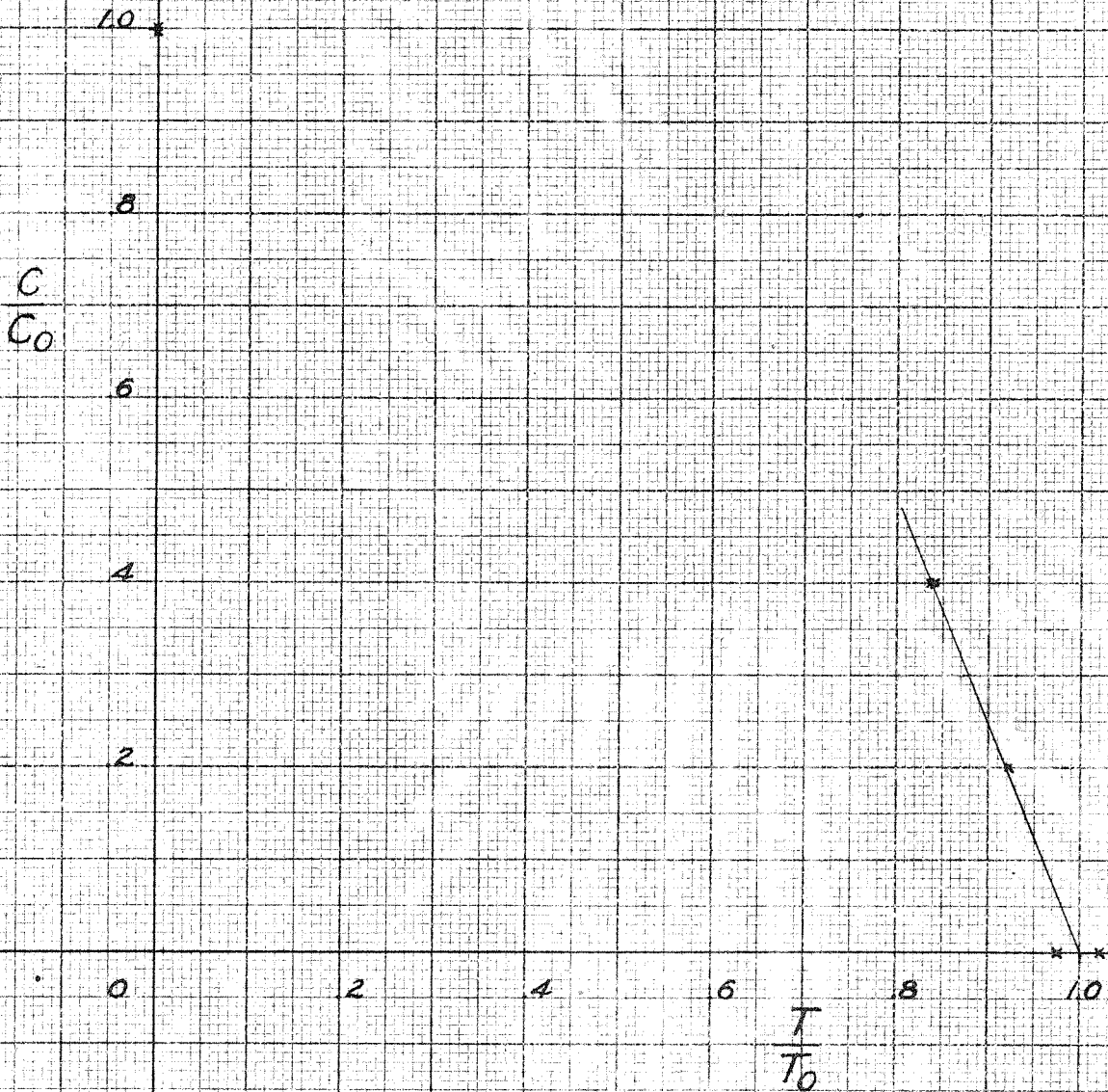
COMPRESSION VS. TORSION
 TEST NO. 9 SPRING BRASS
 $T = 0.066$ $N = 4.1$



COMPRESSION VS. TORSION

TEST NO. 10 - SOFT BRASS

$T = .0053$ $N = 2.5$



COMPRESSION VS TORSION

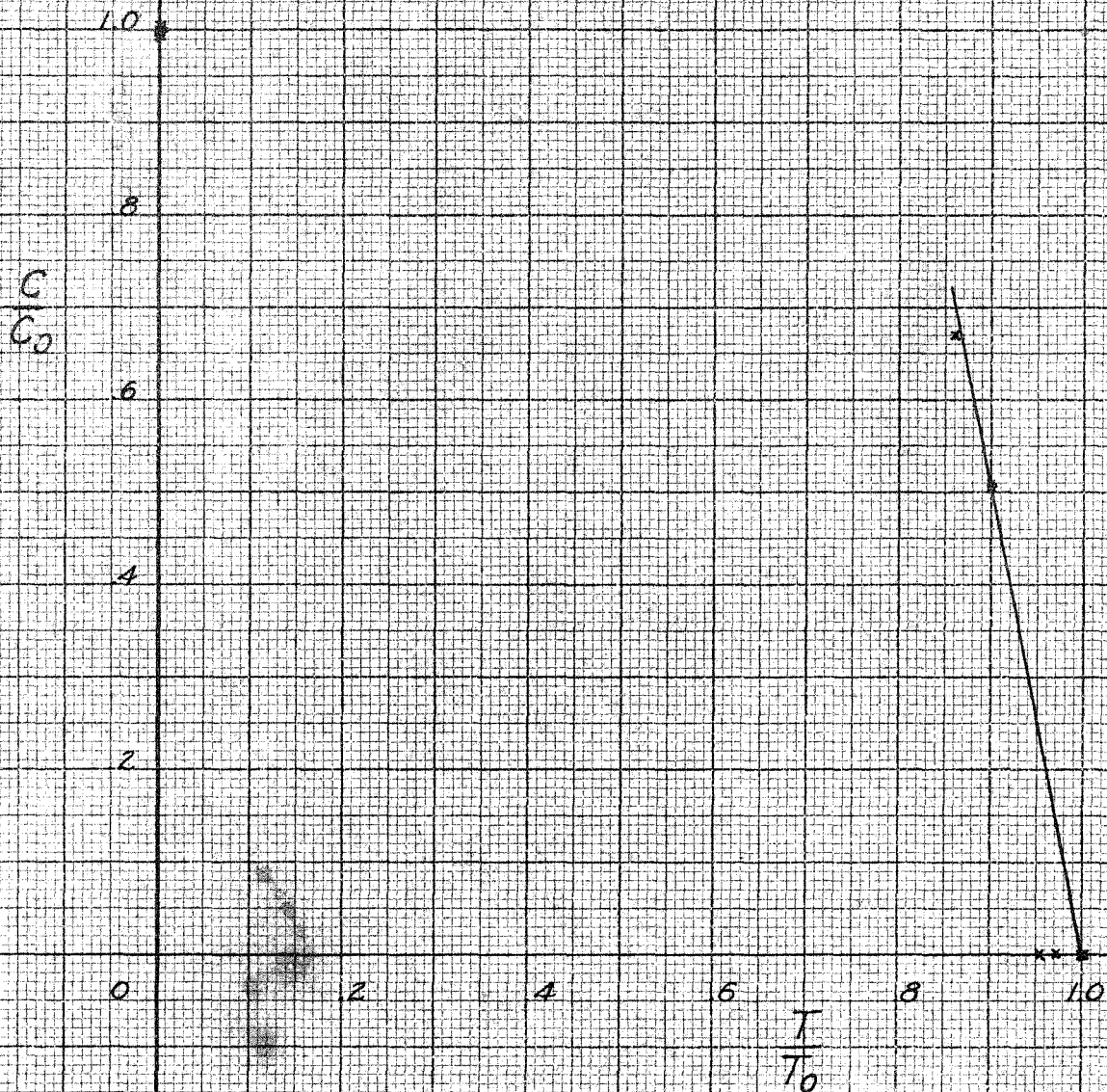
TEST NO. 11

SOFT COPPER

$T = 0.113$

$N = 5.0$

$D = 1.88$



COMPRESSION VS TORSION

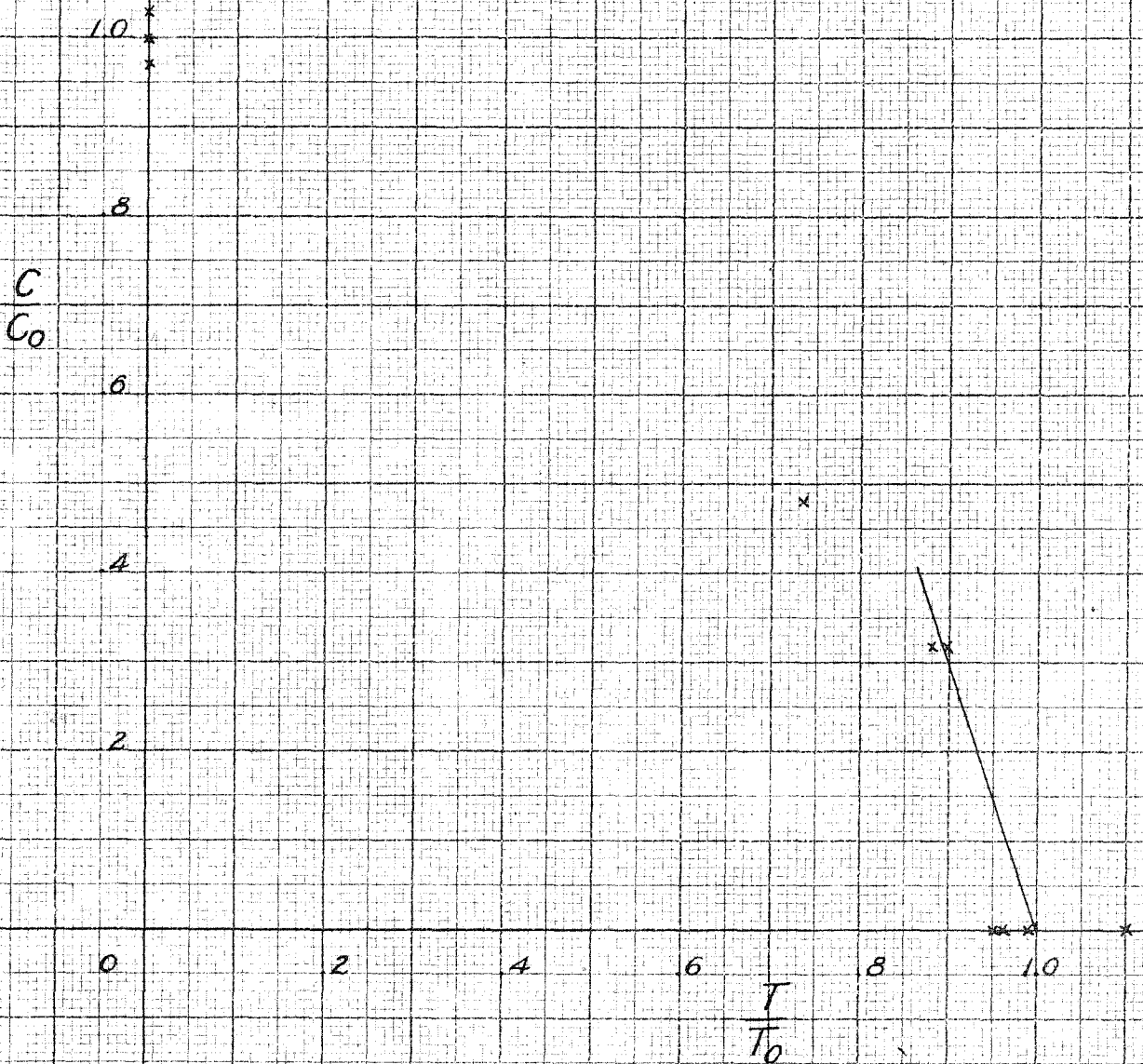
TEST NO. 12

ZINC

$T = .0062$

$N = 3.0$

$D = 1.88$

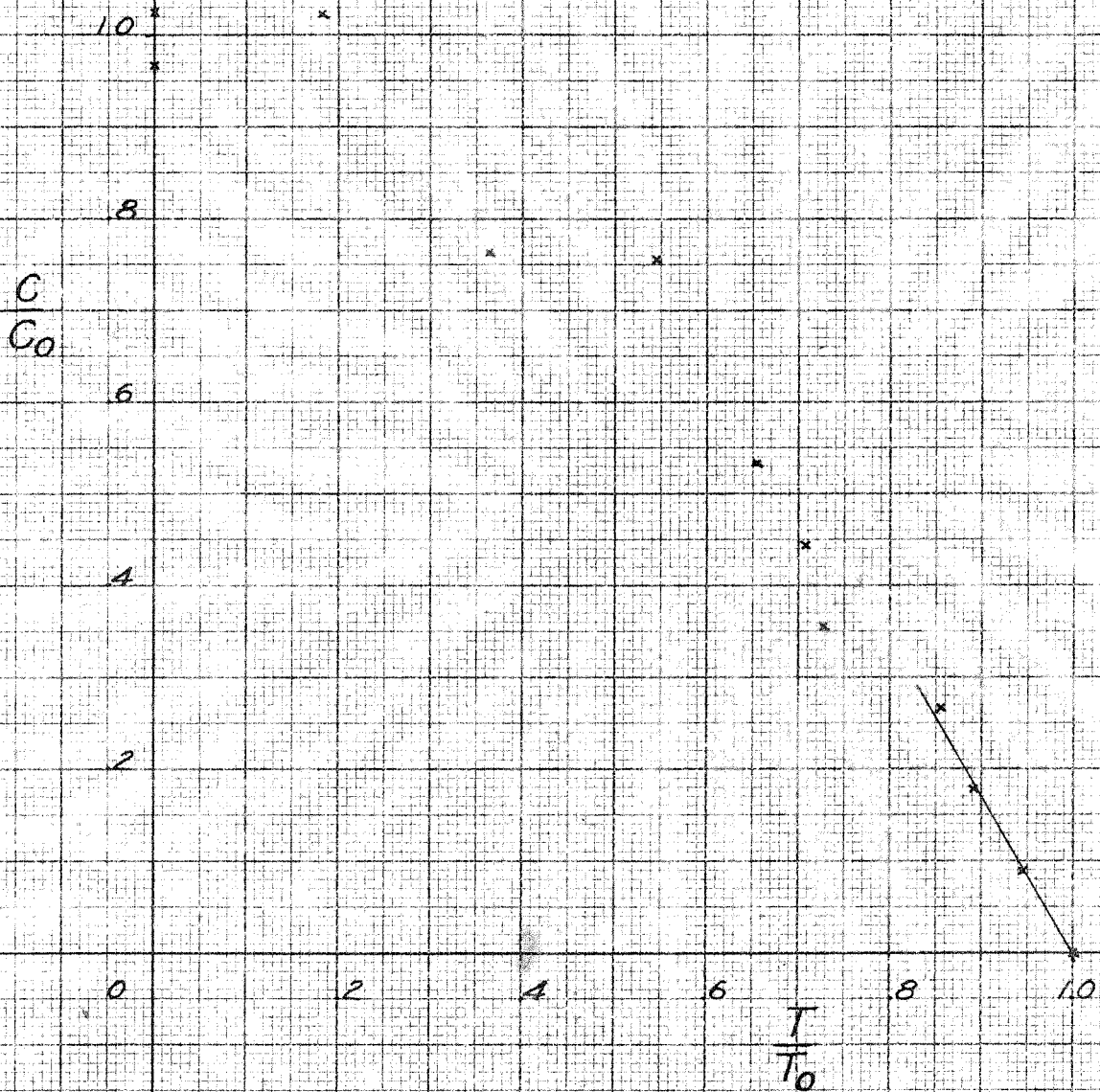


COMPRESSION VS. TORSION

TEST NO. A STEEL

T = 0020 N = 1.8

D = 1.88

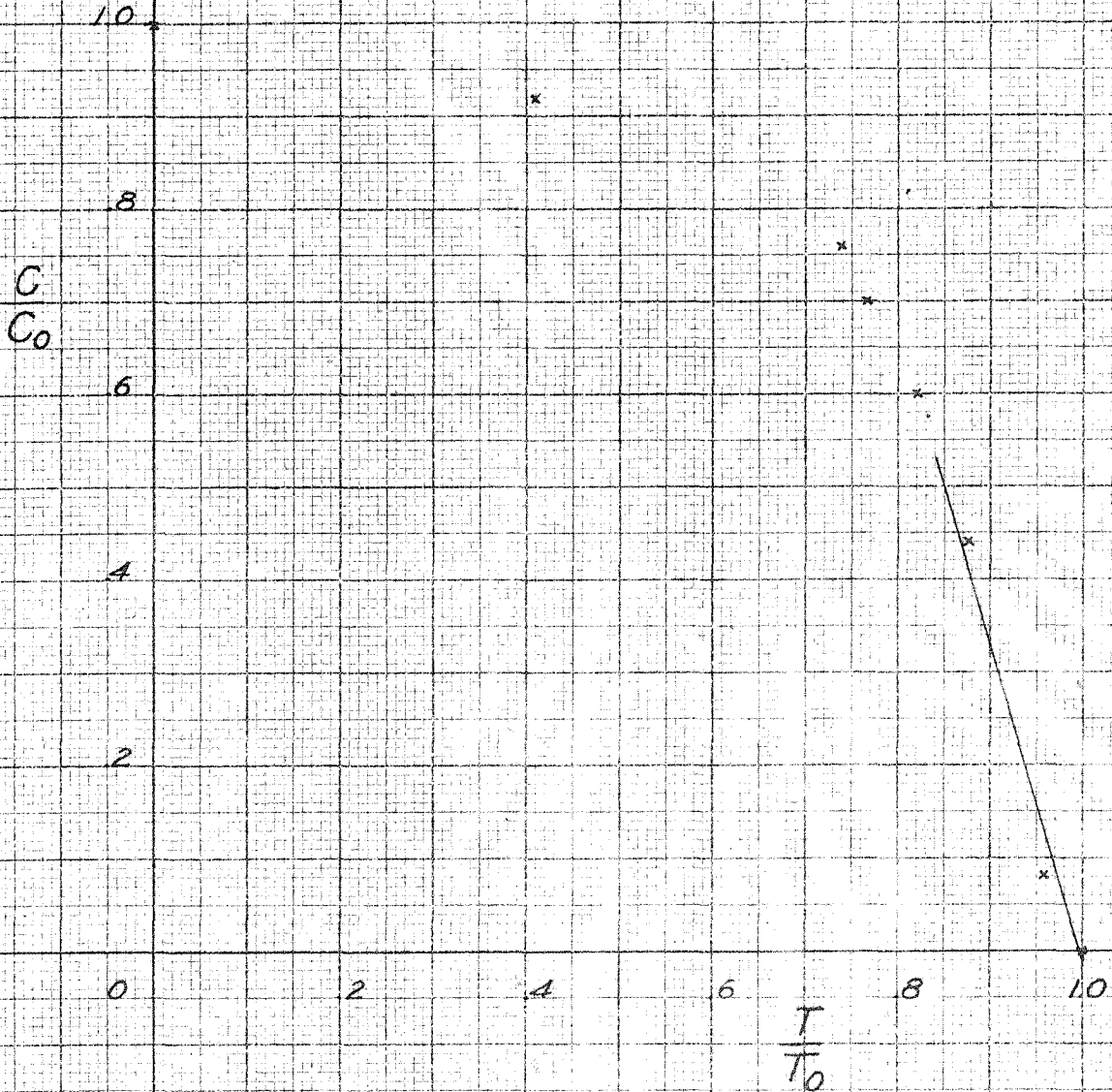


COMPRESSION VS. TORSION

TEST NO. B. BRASS

$T = .0032$ $N = 3.3$

$D = 1.88$

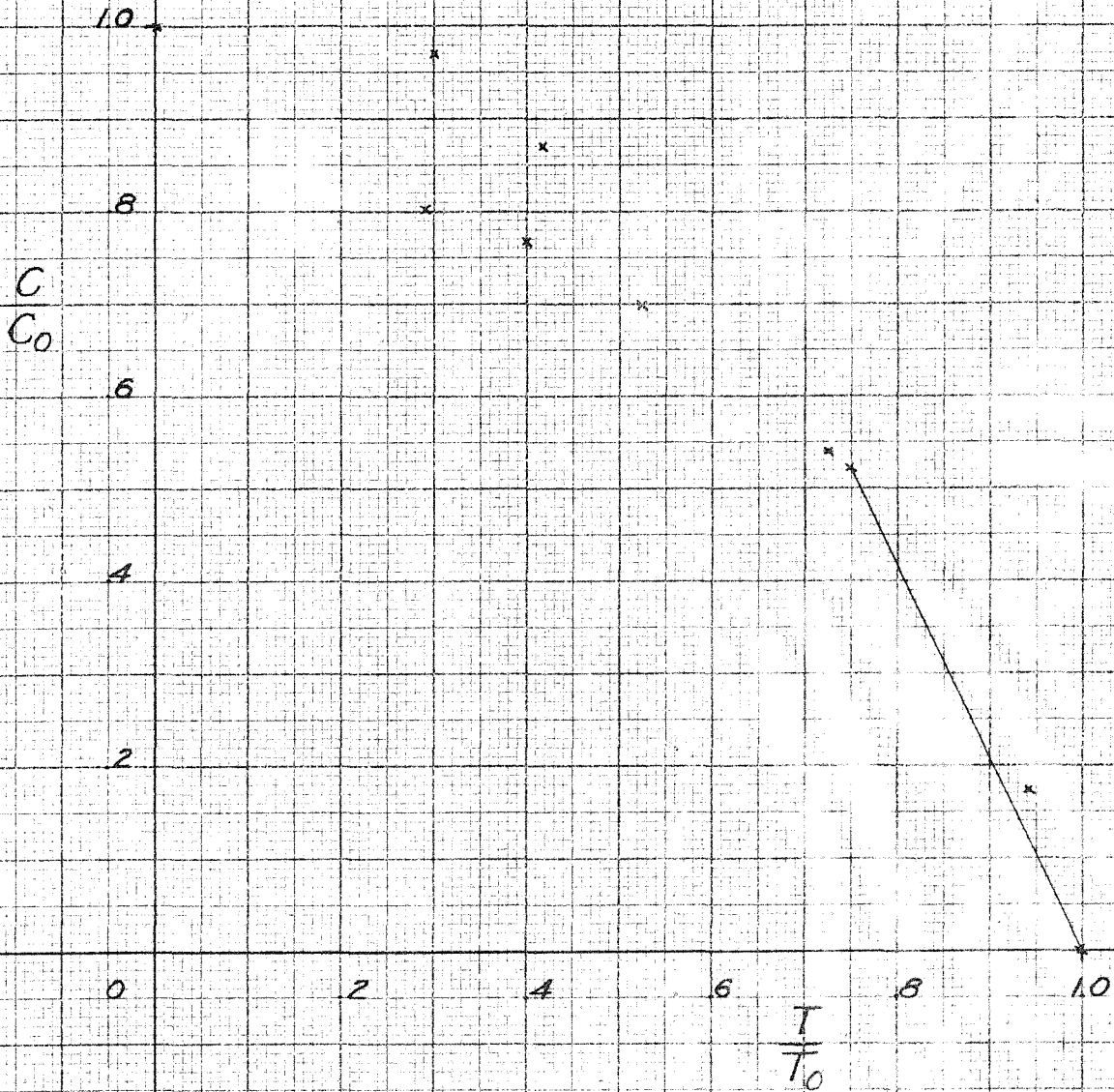


COMPRESSION VS. TORSION

TEST NO. C STEEL

$T = .0030$ $N = 2.1$

$D = 3.75$

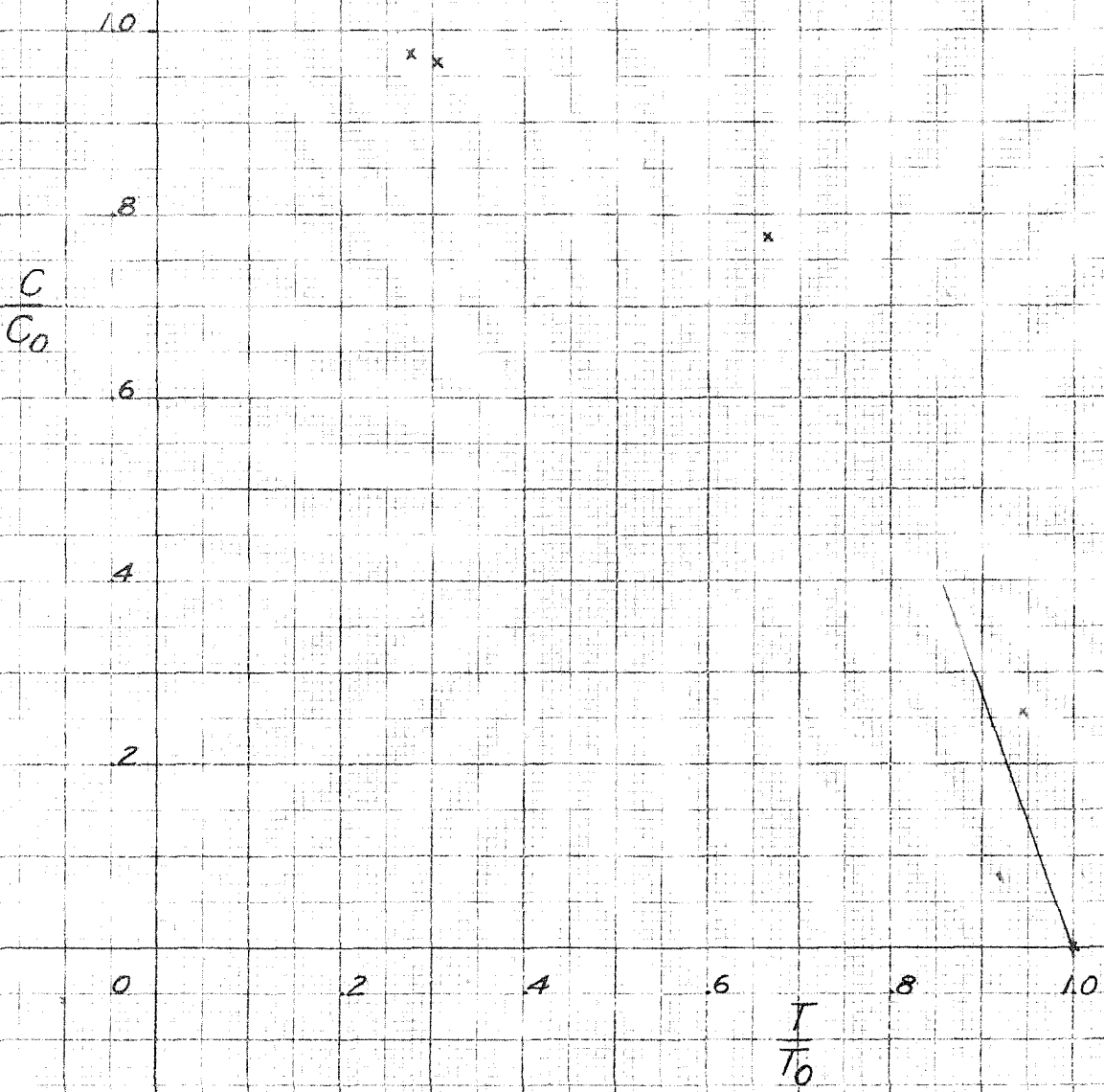


COMPRESSION VS. TORSION

TEST NO. D STEEL

T = .0020 N = 27

DIA. = 1.88

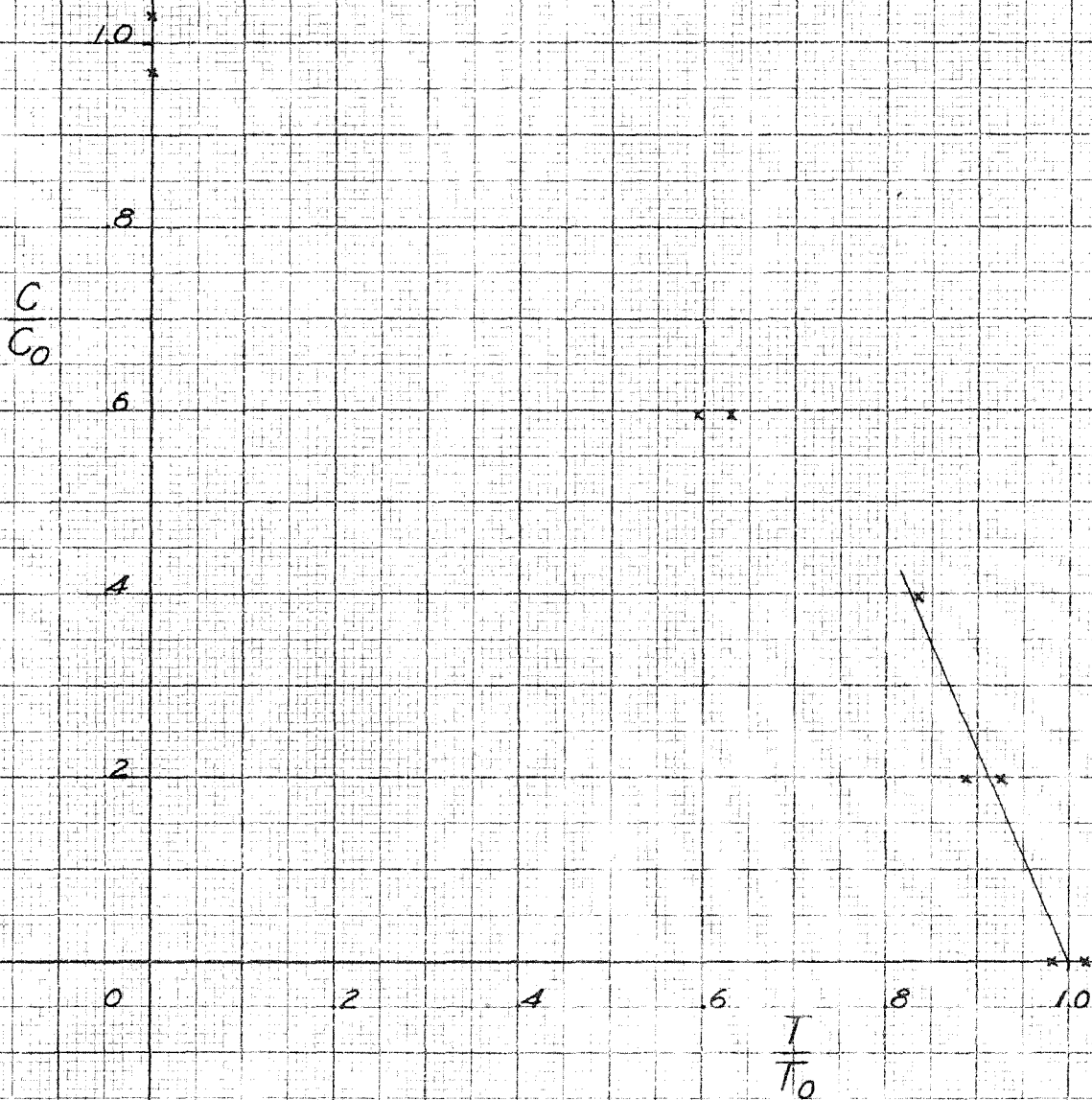


COMPRESSION VS. TORSION

TEST NO. E STEEL

$T = .0030$ $N = 2.3$

$D = 1.88$



COMPRESSION VS TORSION

TEST NO. F STEEL

T = 0020 N = 2.2

D = 3.75

